Stochastic bi-level coordination of active distribution network and renewable-based microgrid considering eco-friendly compressed air energy storage system and intelligent parking lot

Author(s): Haghifam, Sara; Najafi-Ghalelou, Afshin; Zare, Kazem; Shafie-khah, Miadreza; Arefi, Ali

Title: Stochastic bi-level coordination of active distribution network and renewable-based microgrid considering eco-friendly compressed air energy storage system and intelligent parking lot

Year: 2020

Version: Final draft (post print, aam, accepted manuscript)

Please cite the original version:

Haghifam, S., Najafi-Ghalelou, A., Zare, K., Shafie-khah, M., & Arefi, A., (2020). Stochastic bi-level coordination of active distribution network and renewable-based microgrid considering eco-friendly compressed air energy storage system and intelligent parking lot. Journal Vol(number), pp-pp. https://doi.org/10.1007/s11628-018-0361-1

Stochastic Bi-Level Coordination of Active Distribution Network and Renewable-based Microgrid considering Eco-Friendly Compressed Air Energy Storage System and Intelligent Parking Lot

Sara Haghifam[1], Afshin Najafi-Ghalelou[1], Kazem Zare[1,*], Miadreza Shafie-khah[2], Ali Arefi[3]

[1] Faculty of Electrical and Computer Engineering, University of Tabriz, Tabriz, Iran
[2] School of Technology and Innovations, University of Vaasa, Vaasa, Finland
[3] School of Engineering and Information Technology, Murdoch University, Australia
s_haghifam@tabrizu.ac.ir, afshin.najafi95@ms.tabrizu.ac.ir, kazem.zare@tabrizu.ac.ir, mshafiek@uva.fi, a.arefi@murdoch.edu.au
*corresponding author

Abstract

The optimal operation of active distribution systems in the presence of private renewable-based entities is one of the primary challenges of future power networks. In this regard, developing a practical framework to deal with this kind of issue is essential. Hence, in this paper, a novel bi-level stochastic programming approach is presented for optimal energy and reserve scheduling of the active distribution system in the presence of different eco-efficient autonomous players. In the proposed model, the distribution system operator, as a leader, attempts to minimize its total operating costs. At the same time, the renewable-based microgrid owner, as an independent follower, tends to maximize its profit from exchanging energy and reserve with the distribution system operator. The suggested scheme is a non-linear bi-level problem which is transformed into a non-linear single-level problem through Karush–Kuhn–Tucker conditions. In order to find the global optima, the non-linear single-level problem is linearized by utilizing the Big-M method. Finally, to investigate the effectiveness of the provided model, it is tested on the modified IEEE 15-Bus active distribution system under different cases and scenarios. Obtained results indicate that the operation cost of the distribution system operator can be reduced up to 134.09$, from 10710.11$ to 10576.02$, and the profit of the microgrid owner can be increased significantly 906.93$, from 659.455$ to 1566.39$, by considering both environmentally friendly units, IPL and CAES.

Keywords: Stochastic bi-level programming; Active distribution network; Private microgrid owner; Intelligent parking lot; Compressed air energy storage system; Renewable-based microgrid.

Nomenclature

Acronyms	
ADS	Active Distribution System
CAES	Compressed Air Energy Storage
DR	Demand Response
DG	Dispatchable Generators
DSO	Distribution System Operator
DER	Distributed Energy Resource
IPL	Intelligent Parking Lot
KKT	Karush–Kuhn–Tucker
MG	Microgrid
MGO	Microgrid Owner
PDF	Probability Distribution Function
PV	Photovoltaic System
WT	Wind Turbine
Indices	
b , b'	Index of Buses
$\overline{i}$, $\overline{I}$	Index of the upper-level's dispatchable units
$\underline{i}$, $\underline{I}$	Index of the lower-level's dispatchable units
$\overline{j}$, $\overline{J}$	Index of the upper-level's CAES
$\underline{j}$, $\underline{J}$	Index of the lower-level's existed EVs in the IPL
$\overline{k}$, $\overline{K}$	Index of the upper-level's WTs
$\underline{k}$, $\underline{K}$	Index of the lower-level's WTs
$\overline{n}$	Auxiliary index for linear modeling of the upper-level's $\overline{i}^{\,th}$ dispatchable unit
$\overline{p}$, $\overline{P}$	Index of the upper-level's PVs
$\underline{p}$, $\underline{P}$	Index of the lower-level's PVs
s , S	Index of scenarios
t , T	Index of time
Γ	Index of lines
Parameters	
$A_{\overline{i}}^{\mathrm{u}}$, $B_{\overline{i}}^{\mathrm{u}}$	Coefficients of the cost function of the upper-level's $\overline{i}^{\,th}$ dispatchable unit (\$/MWh), (\$/h)
$B_{\underline{i}}^{\mathrm{l}}$	Generation cost of the lower-level's $\underline{i}^{\,th}$ dispatchable unit (\$/MWh)
$b_{\overline{j}}^{\mathrm{inj}}$, $b_{\overline{j}}^{\mathrm{p}}$	Efficiency of the injected/pumped power to/from the $\overline{j}^{\,th}$ CAES (%)
$\overline{G}_{\mathrm{t,s}}^{\mathrm{u}}$	Solar irradiation of the upper-level at time t in scenario s (W/m^2)
$\underline{G}_{\mathrm{t,s}}^{\mathrm{l}}$	Solar irradiation of the lower-level at time t in scenario s (W/m^2)
$HR_{\overline{j}}^{\mathrm{p}}$	Heat rate of the $\overline{j}^{\,th}$ CAES in the pumping mode (MMBtu/MWh)
$\kappa_{\overline{k}}$, $\kappa_{\underline{k}}$	Number of upper/lower-level's WT
$\kappa_{\overline{p}}$, $\kappa_{\underline{p}}$	Number of upper/lower-level's PV

$MUT_{\overline{i}}$, $MDT_{\overline{i}}$	Minimum up/down-time of the upper-level's $\overline{i}^{th}$ dispatchable unit (h)
N^{max}	Maximum number of switching between charging and discharging modes during the presence of each EV in the IPL
$P^{DSO's\,demand}_{t,s}$	The DSO's load demand at time t in scenario s (MW)
$P^{MGO's\,demand}_{t,s}$	The MGO's load demand at time t in scenario s (MW)
$P^{Energy\,Exch,max}_{t,s}$	Maximum level of exchanged power between the MGO and DSO (MW)
$P^{Reserve\,Exch,max}_{t,s}$	Maximum level of exchanged reserve between the MGO and DSO (MW)
$PL^{max}_{b,b',t,s}$	Maximum capacity of the line between the b^{th} and b'^{th} buses (MW)
$\overline{P}^{UG,max}_{t,s}$	Limitation of exchanged power between the DSO and the wholesale market (MW)
$\underline{P}^{UG,max}_{t,s}$	Limitation of exchanged power between the MG and the retail market (MW)
$P^{rated}_{\overline{k}}$, $P^{rated}_{\underline{k}}$	Rated power of the upper/lower-level's $\overline{k}^{th}$/$\underline{k}^{th}$ WT (MW)
$\overline{P}^{max}_{\overline{i}}$, $\overline{P}^{min}_{\overline{i}}$	The maximum/minimum output power of the upper level's $\overline{i}^{th}$ dispatchable unit (MW)
$\underline{P}^{max}_{\underline{i}}$, $\underline{P}^{min}_{\underline{i}}$	The maximum/minimum output power of the lower-level's $\underline{i}^{th}$ dispatchable unit (MW)
$P^{Ch,max}_{\underline{j}}$, $P^{Dch,max}_{\underline{j}}$	Maximum charging/discharging power of the $\underline{j}^{th}$ EV (MW)
$RU^{L}_{\underline{i}}$, $RD^{L}_{\underline{i}}$	Ramp up/down rate of the lower-level's $\underline{i}^{th}$ dispatchable unit (MW/h)
$RU^{U}_{\overline{i}}$, $RD^{U}_{\overline{i}}$	Ramp up/down rate of the upper-level's $\overline{i}^{th}$ dispatchable unit (MW/h)
$s_{\overline{p}}$, $s_{\underline{p}}$	Area of the upper/lower-level's PV system (m^2)
$\overline{S}^{uc}_{\overline{i}}$, $\overline{S}^{dc}_{\overline{i}}$	Start-up/shut-down cost of the upper-level's $\overline{i}^{th}$ dispatchable unit ($)
$\underline{S}^{uc}_{\underline{i}}$	Start-up cost of the lower-level's $\underline{i}^{th}$ dispatchable unit ($)
$SOC^{CAES,max}_{\overline{j},t,s}$	Maximum amount of stored energy in the $\overline{j}^{th}$ CAES (MWh)
$SOC^{CAES,min}_{\overline{j},t,s}$	Minimum amount of stored energy in the $\overline{j}^{th}$ CAES (MWh)
$SOC^{Arrival}_{\underline{j}}$	The initial amount of stored energy in the $\underline{j}^{th}$ EV (MWh)
$SOC^{IPL,max}_{\underline{j}}$	Maximum amount of stored energy in the $\underline{j}^{th}$ EV (MWh)
$SOC^{IPL,min}_{\underline{j}}$	Minimum amount of stored energy in the $\underline{j}^{th}$ EV (MWh)
$TU_{\overline{i},n}$, $TD_{\overline{i},n}$	Auxiliary parameter for the minimum up/down-time limit of the upper-level's $\overline{i}^{th}$ dispatchable unit
$t^{Arv.}$, $t^{Dep.}$	The EVs arrival/departure time to/from the IPL (h)
t^{min} , t^{max}	Minimum/maximum presence time of EV's in the IPL (h)
$\overline{V}_{t,s}$, $\underline{V}_{t,s}$	Wind speed of the upper/lower-level at time t in scenario s (m/s)
$V^{rated}_{\overline{k}}$, $V^{rated}_{\underline{k}}$	Rated speed of the upper/lower-level's $\overline{k}^{th}$/$\underline{k}^{th}$ WT (m/s)
$V^{cut-in}_{\overline{k}}$, $V^{cut-out}_{\overline{k}}$	The cut-in/cut-out speed of the upper-level's $\overline{k}^{th}$ WT (m/s)
$V^{cut-in}_{\underline{k}}$, $V^{cut-out}_{\underline{k}}$	The cut-in/cut-out speed of the lower-level's $\underline{k}^{th}$ WT (m/s)
$V^{inj,min}_{\overline{j}}$, $V^{inj,max}_{\overline{j}}$	Minimum/maximum limitation of injecting air to the $\overline{j}^{th}$ CAES (MW/h)
$V^{p,min}_{\overline{j}}$, $V^{p,max}_{\overline{j}}$	Minimum/maximum limitation of pumping air to the combustion chamber of the $\overline{j}^{th}$ CAES (MW/h)
$vom^{inj}_{\overline{j}}$, $vom^{p}_{\overline{j}}$	Operation and maintenance cost of the $\overline{j}^{th}$ CAES in the injecting/pumping mode ($/MWh)
$X_{b,b'}$	Reactance of the line between b^{th} and b'^{th} buses

$\underline{\lambda}_{j}^{\text{Ch,EV}}$	Charging price of the $\underline{j}^{th}$ EV ($/MWh)
$\underline{\lambda}_{j}^{\text{Dch,EV}}$	Discharging price of the $\underline{j}^{th}$ EV ($/MWh)
$\lambda_{t}^{\text{Energy Exch}}$	Bilateral contract tariff between the DSO and MGO at time t for exchanging energy ($/MWh)
$\lambda_{t}^{\text{Reserve Exch}}$	Bilateral contract tariff between the DSO and MGO at time t for exchanging reserve ($/MWh)
λ_{g}	Natural gas price ($/MMBtu)
$\overline{\lambda}_{\bar{j}}^{\text{RV,CAES}}$	Price of the scheduled reserve by the upper-level's $\bar{j}^{th}$ CAES system ($/MWh)
$\underline{\lambda}_{j}^{\text{RV,EV}}$	Price of the scheduled reserve by the lower-level's $\underline{j}^{th}$ EV ($/MWh)
$\overline{\lambda}_{\bar{i}}^{\text{RV,DG}}$	Price of the scheduled reserve by the upper-level's $\bar{i}^{th}$ dispatchable unit ($/MWh)
$\underline{\lambda}_{i}^{\text{RV,DG}}$	Price of the scheduled reserve by the lower-level's $\underline{i}^{th}$ dispatchable unit ($/MWh)
$\overline{\lambda}_{t,s}^{\text{UG}}$, $\underline{\lambda}_{t,s}^{\text{UG}}$	The wholesale/retail market price at time t in scenario s ($/MWh)
$\overline{\omega}_{\text{wind}}$, $\underline{\omega}_{\text{wind}}$	Forecasting errors of the upper/lower-level's wind speed (%)
$\overline{\omega}_{\text{solar}}$, $\underline{\omega}_{\text{solar}}$	Forecasting errors of the upper/lower-level's solar irradiation (%)
$\overline{\omega}_{\text{load}}$, $\underline{\omega}_{\text{load}}$	Forecasting errors of the upper/lower-level's load demand (%)
$\pi_{t,s}$	Probability of each scenario at time t
$\eta_{\bar{p}}$, $\eta_{\underline{p}}$	Conversion efficiency of the upper/lower-level's solar cells (%)
η^{g2v} , η^{v2g}	Charging/discharging efficiency (%)
ψ	Percentages of the dispatchable units' available capacity for participation in reserve (%)
σ	Percentages of the EVs' available power for participation in reserve (%)
χ	The desired state of charge at the departure time of the $\underline{j}^{th}$ EV from the IPL (%)
$\Delta SOC_{\underline{j}}^{\max}$	Maximum allowable rate of charging/discharging of the $\underline{j}^{th}$ EV (MWh)
Variables	
$\overline{\text{Cost}}_{t,s}^{\text{CAES}}$	Operating costs of the upper-level's CAES at time t in scenario s ($/h)
$\overline{\text{Cost}}_{t,s}^{\text{DG}}$	Operating costs of the upper-level's dispatchable units at time t in scenario s ($/h)
$\underline{\text{Cost}}_{t,s}^{\text{DG}}$	Operating costs of the lower-level's dispatchable units at time t in scenario s ($/h)
$P_{\bar{k},t,s}^{\text{WT}}$, $P_{\underline{k},t,s}^{\text{WT}}$	Produced power by the upper/lower-level's $\bar{k}^{th}$/ $\underline{k}^{th}$ WT at time t in scenario s (MW)
$P_{\bar{p},t,s}^{\text{PV}}$, $P_{\underline{p},t,s}^{\text{PV}}$	Produced power by the upper/lower-level's $\bar{p}^{th}$/ $\underline{p}^{th}$ PV at time t in scenario s (MW)
$P_{t,s}^{\text{Energy Exch}}$	Exchanged power between the DSO and MGO at time t in scenario s (MW)
$P_{t,s}^{\text{Reserve Exch}}$	Exchanged reserve between the DSO and MGO at time t in scenario s (MW)
$\overline{P}_{t,s}^{\text{UG}}$	Exchanged power between the DSO and the wholesale market at time t in scenario s (MW)
$\underline{P}_{t,s}^{\text{UG}}$	Exchanged power between the MGO and the retail market at time t in scenario s (MW)
$P_{\bar{i},t,s}^{\text{DG}}$	Produced power by the upper level's $\bar{i}^{th}$ dispatchable unit at time t in scenario s (MW)
$P_{\bar{i},t,s}^{\text{RV,DG}}$	Scheduled reserve by the upper level's $\bar{i}^{th}$ dispatchable unit at time t in scenario s (MW)
$P_{\underline{i},t,s}^{\text{DG}}$	Produced power by the lower-level’s $\underline{i}^{th}$ dispatchable unit at time t in scenario s (MW)
$P_{\underline{i},t,s}^{\text{RV,DG}}$	Scheduled reserve by the lower-level's $\underline{i}^{th}$ dispatchable unit at time t in scenario s (MW)
$P_{\bar{j},t,s}^{\text{cs}}$	Produced power by the $\bar{j}^{th}$ CAES at time t in scenario s(MW)

$P^{cp}_{\bar{j},t,s}$	Consumed power by the $\bar{j}^{th}$ CAES at time t in scenario s (MW)
$P^{RV,CAES}_{\bar{j},t,s}$	Scheduled reserve by the $\bar{j}^{th}$ CAES at time t in scenario s (MW)
$P^{Ch,EV}_{\underline{j},t,s}$	Charge rate of the $\underline{j}^{th}$ EV at time t in scenario s (MW)
$P^{Dch,EV}_{\underline{j},t,s}$	Discharged rate of the $\underline{j}^{th}$ EV at time t in scenario s (MW)
$P^{RV,EV}_{\underline{j},t,s}$	Scheduled reserve by the $\underline{j}^{th}$ EV at time t in scenario s (MW)
$PI^{En}_{b,t,s}$, $PI^{Re}_{b,t,s}$	Total injected power/reserve to the b^{th} bus at time t in scenario s (MW)
$PL^{En}_{b,b',t,s}$, $PL^{Re}_{b,b',t,s}$	Active power/reserve flow between the b^{th} and b'^{th} nodes at time t in scenario s (MW)
$PL_{b,b',t,s}$	Total power flow between the b^{th} and b'^{th} nodes at time t in scenario s (MW)
$SUC_{\bar{i},t,s}$, $SDC_{\bar{i},t,s}$	Start-up/shut-down cost of the upper-level's $\bar{i}^{th}$ dispatchable unit at time t in scenario s ($)
$SUC_{\underline{i},t,s}$	Start-up cost of the lower-level's $\underline{i}^{th}$ dispatchable unit at time t in scenario s ($)
$SOC^{CAES}_{\bar{j},t,s}$	Amount of stored energy in the $\bar{j}^{th}$ CAES at time t in scenario s (MWh)
$SOC^{IPL}_{\underline{j},t,s}$	Amount of stored energy in the $\underline{j}^{th}$ EV at time t in scenario s (MWh)
$V^{inj}_{\bar{j},t,s}$	The energy equivalent of injected air to the $\bar{j}^{th}$ CAES at time t in scenario s (MWh)
$V^{p}_{\bar{j},t,s}$	The energy equivalent of pumped air into the combustion chamber at time t in scenario s (MWh)
$\delta^{En}_{b,t,s}$, $\delta^{Re}_{b,t,s}$	Voltage angles at node b, time t, and in scenario s (rad)
λ , μ	Dual variables
Binary variables	
$M_{\underline{j},t}$	Binary variable; Equal to 1 if the $\underline{j}^{th}$ EV be in the parking lot; otherwise 0
$SRS_{\underline{j},t,s}$	Binary variable; Equal to 1 if the $\underline{j}^{th}$ EV participates in the reserve; otherwise 0
$U^{inj}_{\bar{j},t,s}$	Binary variable; Equal to 1 if the air is injected to the $\bar{j}^{th}$ CAES at time t in scenario s; otherwise 0
$U^{p}_{\bar{j},t,s}$	Binary variable; Equal to 1 if the air is pumped from the $\bar{j}^{th}$ CAES at time t in scenario s; otherwise 0
$V^{DG}_{\bar{i},t,s}$	Binary variable; Equal to 1 if the upper-level's $\bar{i}^{th}$ dispatchable unit be ON at time t in scenario s; otherwise 0
$V^{DG}_{\underline{i},t,s}$	Binary variable; Equal to 1 if the lower-level's $\underline{i}^{th}$ dispatchable unit be ON at time t in scenario s; otherwise 0
$W^{Ch}_{\underline{j},t,s}$	Binary variable; Equal to 1 if the $\underline{j}^{th}$ EV be in the charge mode; otherwise 0
$W^{Dch}_{\underline{j},t,s}$	Binary variable; Equal to 1 if the $\underline{j}^{th}$ EV be in the discharge mode; otherwise 0
X	Binary variable for linearization of the complementary conditions

1. Introduction

Recently, with high penetration of Distributed Energy Resources (DER), including Wind Turbines (WT), Dispatchable Generators (DG), micro-turbines, energy storage systems [1], and Photovoltaic Systems (PV), electricity networks have been changed from passive distribution systems into the Active Distribution Systems (ADS) [2]. On the other hand, in order to optimal control and support these kinds of energy resources, the Microgrid (MG) concept has been introduced [3]. By increasing the number of MGs and emergence of new environmentally-responsible infrastructures such as Intelligent Parking Lots (IPL) in the ADSs, Microgrid Owners (MGO), as private entities, have taken responsibility for managing these local units. It should be noted that IPL plays the role of an aggregator that facilitates interaction between EVs owners and MGOs. Being variable in the amount of the stored energy during different periods can be considered as the main difference between the IPL and the conventional energy storage systems [4]. However, these new players follow conflicting objectives as opposed to the Distribution System Operators (DSO). This matter has resulted in a competitive environment among the entire independent financial players. Based on these realities, the DSOs are faced with fundamental challenges in terms of optimal scheduling of their networks. So, to meet the mentioned problems, the DSOs have to interact and trade with these sorts of players in an efficient way [5]. Hence, proposing an appropriate method in which all participants could achieve a high amount of profit is vital. As a result, in this paper, it has been attempted to present a framework based on the Game Theory for energy and reserve management of the ADS in the presence of a private MGO. The provided model in this paper is the bi-level programming problem that minimizes the DSO's total operating costs in the upper-level and maximizes the MGO's benefit in the lower-level considering the capability of exchanging the scheduled energy and reserve with each other through bilateral contracts. Furthermore, uncertainties of electricity prices, load demand, and output power of renewable energy sources are other crucial issues that should be taken into account by the system operators. Consequently, in this article, it has been tried to implement a scenario-based stochastic programming method to handle the mentioned uncertainty parameters.

1.1. Literature Review

Studied relevant articles in the field of the single-level optimization models can be summarized as follows: The day-ahead scheduling of MGs has been provided in [6] to minimize their operating costs under the EV aggregator constraints. The deterministic-based models of the WT and PV have been considered in the mentioned paper. In order to minimize the operation cost of the smart distribution network and EV aggregators that cooperated, a decentralized robust optimization approach has been provided in [7]. The uncertainties of the market price and wind speed are taken into account in this study, too. A novel stochastic optimization-based energy and reserve scheduling model of the MG has been presented in [8] to minimize the total costs of the studied system under different types of demand response (DR) programs and uncertainties of the solar irradiation and wind speed. In order to minimize the energy and reserve costs of a smart distribution system under the wind speed and electric demand uncertainties, a new two-point estimate method has been provided in [9]. A novel day-ahead stochastic optimization approach-based model has been proposed in [10] for joint energy and reserve scheduling under incentive-based DR programs and wind speed uncertainty. In order to minimize the operation cost of the distribution networks and private MGs that cooperated, a decentralized adaptive robust optimization approach has been suggested in [11]. The uncertainties of market price, wind speed, and solar irradiation are considered in this work, too. To maximize the profit of the smart distribution company that consists of renewable energy sources and a parking lot, a novel techno-economic model has been proposed in [12]. The effects of different price/incentive-based DR programs, as well as the uncertainties of the EVs, wind speed, and solar irradiation, are investigated in this study, too. A novel risk-based market-clearing framework has been provided in [13] to clear the joint reserve and energy markets in power and gas systems considering the CAES and WTs constraints. The uncertainty of wind speed is considered in the mentioned paper. A new plug-in EV model has been presented in [14] to minimize the operation costs of the ADSs and reduce the CO_2 emission and congestion under the time-based DR program. The uncertainties of renewable energy resources and travel patterns of plug-in EVs are studied in this paper, as well. A deterministic multi-objective model has been exploited in [15] to investigate the economic-environmental operation of solar-based IPLs in the presence of the time-of-use DR program. In the mentioned paper, the IPL's total operating cost, as well as the generated greenhouse gases, have been minimized. A mixed-integer non-linear programming model has been developed in [16] to solve the renewable-based MG model that quipped with varied DERs and a parking lot. Finally, the mixed-integer non-linear programming-based framework has been provided in [17] to model the participation of several EVs, dispatchable resources, and non-dispatchable units as a joint aggregator in the electricity market. The objective function of this aggregator is to maximize its profit in an uncertain environment.

Studied relevant papers in the field of the bi-level optimization models can be summarized as follows: A novel bi-level optimization method has been conducted in [18] to maximize the profit of the smart distribution company and the parking lot owner. Also, the uncertainties of the wind speed, solar irradiation, market price, and parking lot constraints are considered in this paper. A bi-level strategy has been implemented in [19] to minimize the total operation cost of the DSO and maximize the profit of multi-MGs. Moreover, the uncertainties of the solar irradiation, market price, and electric demand are considered in this paper. To maximize the profit of the distribution company and simultaneously minimize the operation cost of several MGs under the power exchange capability, a bi-level optimization approach has been presented in [20]. A deterministic multi-objective-based bi-level model has been provided in [21] to minimize the power loss and improve the voltage profile of the distribution networks as well as minimize the operation costs of multi-MGs that play the role of followers. To maximize the benefit of the DSOs and the parking lot owners under the uncertain behavior of the EV owners, a novel dynamic bi-level model has been suggested in [22]. A risk-constraint environmental-based bi-level model has been implemented in [23] to maximize the profit of a distribution company and the parking lot owner under different kinds of DR programs. The uncertainties of wind speed, solar irradiation, and EVs are considered in this work, too. A bi-level programming model has been presented in [24] to maximize the profit of the virtual power plants and minimize the system's operation costs under wind speed and solar irradiation uncertainties. A deterministic-based multi-follower bi-level optimization model has been provided in [25] to analyze the power exchange capability between the distribution network operators and several MGs under the DR program constraints. A stochastic-based multi-follower bi-level model has been investigated in [26] to solve the combined heat and power-based MGs under the uncertainties of wind speed, electric demand, market price, and DR program constraints. Ultimately, A bi-level model has been provided in [27] to minimize the operation costs under the capability of energy and reserve interaction between the DSO and the IPL. The uncertainties of the wind speed and electric demand are taken into account in the mentioned paper, as well. The main structure of reviewed papers can be highlighted as follows:

Table 1: Comparison between the current paper and previous studies.

Ref.	Bi-Level Programming	Reserve Commitment	Uncertainty Modeling	DSO	MGO	IPL	CAES	WT	PV	DG
[6]	✗	✗	✗	✗	✓	✓	✗	✓	✓	✓
[7]	✗	✗	✓	✓	✗	✓	✗	✓	✗	✓
[8]	✗	✓	✓	✗	✓	✗	✗	✓	✓	✓
[9]	✗	✓	✓	✓	✗	✗	✗	✓	✗	✓
[10]	✗	✓	✓	✓	✗	✗	✗	✓	✗	✓
[11]	✗	✗	✓	✓	✓	✗	✗	✓	✓	✓
[12]	✗	✗	✓	✓	✗	✓	✗	✓	✓	✗
[13]	✗	✓	✓	✗	✗	✗	✓	✓	✗	✓
[14]	✗	✗	✓	✓	✗	✓	✗	✓	✓	✓
[15]	✗	✗	✗	✗	✗	✓	✗	✓	✓	✓
[16]	✗	✓	✓	✗	✓	✓	✗	✓	✓	✓
[17]	✗	✗	✓	✗	✗	✓	✗	✓	✓	✓

[18]	✓	×	✓	✓	×	✓	×	✓	✓	×
[19]	✓	×	✓	✓	✓	×	×	×	✓	✓
[20]	✓	×	×	✓	✓	×	×	×	×	✓
[21]	✓	×	✓	✓	✓	×	×	✓	✓	✓
[22]	✓	×	✓	✓	×	✓	×	×	×	×
[23]	✓	×	✓	✓	×	✓	×	✓	✓	×
[24]	✓	✓	✓	×	×	×	×	✓	✓	×
[25]	✓	×	×	✓	✓	×	×	✓	✓	✓
[26]	✓	×	✓	×	✓	×	×	✓	×	✓
[27]	✓	✓	✓	✓	×	✓	×	✓	×	×
Current Paper	✓	✓	✓	✓	✓	✓	✓	✓	✓	✓

1.2. Novelty and Contributions

Reviewing the presented articles depicts that in the bi-level optimization models, simultaneous scheduling of energy and reserve under the distribution network constraints has not been investigated. On the other hand, in provided frameworks, autonomous players of the ADS have not been allowed to take part in different electricity markets such as the retail market. Moreover, in previous works, the impact of the dependent eco-friendly IPL has not been studied on the optimal operation of independent MGOs. So, to fill the mentioned gaps, in this paper, it has been tried to provide a hierarchical decision-making model for optimal energy and reserve scheduling of the ADS in the presence of an independent MGO. The considered ADS is equipped with the CAES and different large-scale dispatchable/renewable-based units. On the other hand, the proposed MG is equipped with the IPL and different small-scale dispatchable/renewable-based units. Also, the uncertainties of various parameters such as wind speed, solar irradiation, market price, and electric demand are considered in the proposed model. According to the above descriptions, the main contributions and novelties of the presented paper can be summarized as follows:

1. Developing the stochastic bi-level programming approach for joint optimal energy and reserve scheduling of the ADS in the presence of a private renewable-based MGO.

2. Proposing a new framework in which the ADS' independent players not only interact with each other but also can participate in separate electricity markets, namely the wholesale and retail markets.
3. Investigating the effects of different resources like the eco-efficient IPL and CAES on the optimal operation of the studied distribution system.

2. Scenario-based Uncertainty Modeling

As mentioned earlier, generally, system operators are confronted with plenty of uncertainties in the optimal scheduling of their networks. In order to study the uncertain nature of these variables, in this work, the scenario-based stochastic programming approach is exploited, which contains two different steps: Scenario Generation and Scenario Reduction. In the following, each stage is described in more detail.

2.1. Scenario Generation

In this paper, the required scenarios are generated based on the Probability Distribution Function (PDF) of stochastic parameters. In this regard, the Normal PDF is used to model uncertainties of the market price and load demand [28]. The Weibull PDF and Beta PDF are considered for uncertainty modeling of wind speed and solar radiation, respectively [29]. The mentioned PDF curves are split into five distinct intervals with the width of the standard deviation that each created area represents one scenario. Figure 1 indicates the discrete form of a typical PDF curve. It should be pointed out that the mean and standard deviation (μ_s , σ_s) of the PDFs are taken from [30, 31].

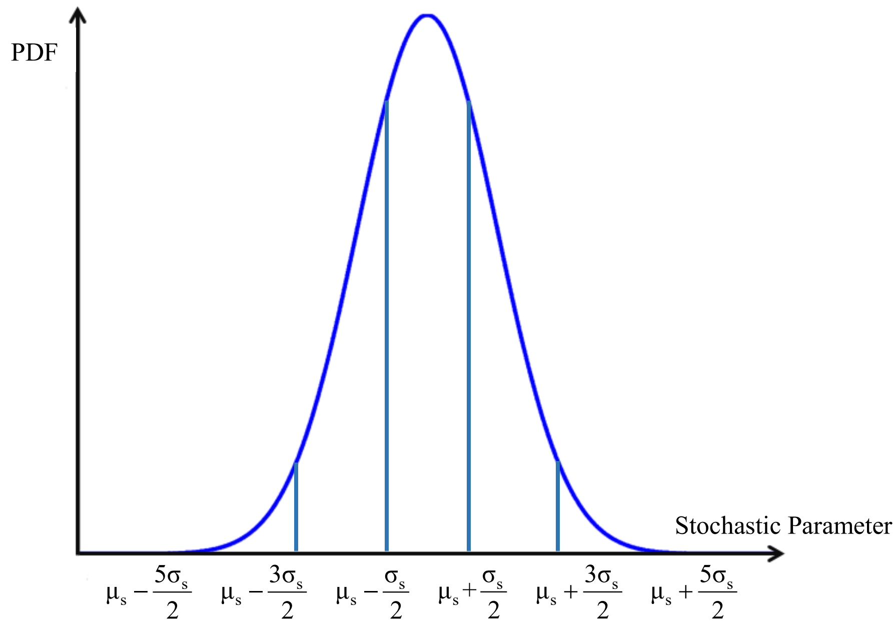

Fig. 1. The PDF of a stochastic parameter and generated scenarios.

2.2. Scenario Reduction

Since a large number of scenarios lead to complexity in the optimization process, the number of them should be reduced. In this article, in order to reduce the number of generated scenarios, the SCENRED2 tool in GAMS software is utilized. At first, all considered independent scenarios are considered as input data of the tree. The constructed tree is in the fan format, and the mixture of fast backward/backward methods is used to reduce the entire number of scenarios to four scenarios. The probabilities of reduced scenarios at each time are provided in Table 1. It is noteworthy that the reduced and selected scenarios contain the features of all scenarios that are entered as input data of the tree. Detailed descriptions regarding the mentioned tree and utilized approach are accessible in Ref. [32].

Table 2: Probability of each scenario at each time.

Scenario 1	Scenario 1	Scenario 1	Scenario 2	Scenario 2	Scenario 2	Scenario 2	
t_1	t_2 - t_4	t_5 - t_{24}	t_1	t_2 - t_3	t_4 - t_8	t_9 - t_{24}	
0.2	0.19	0.21	0.2	0.207	0.225	0.34	
Scenario 3	Scenario 3	Scenario 3	Scenario 3	Scenario 4	Scenario 4	Scenario 4	Scenario 4
t_1	t_2 - t_3	t_4 - t_8	t_9 - t_{24}	t_1	t_2 - t_3	t_4	t_5 - t_{24}
0.2	0.207	0.225	0.11	0.4	0.396	0.36	0.34

3. General Model of the Bi-Level Stochastic Programming Approach

The main goal of this study is to present a suitable framework for optimal energy and reserve scheduling of the ADS in the presence of a private MGO. The existence of this private entity with conflicting objective functions and also the necessity of interaction between the DSO and MGO are led to complexity in the optimization procedure. In order to cope with these types of difficulties, the bi-level stochastic programming model is proposed. In general, the bi-level optimization problem is defined as a special mathematical approach, where one optimization problem is nested within another problem. The outer optimization task is referred to as the upper-level or the leader, while the inner optimization task is referred to as the lower-level or the follower. The outline of the bi-level model can be formulated as follows [33]:

$$\begin{aligned}
&\min_{y,z_1,\ldots,z_m} F_{\text{upper-level}}\left(y,z_1,\ldots,z_m\right)\\
&\qquad \text{s.t:}\begin{cases} G_{\text{upper-level}}\left(y,z_1,\ldots,z_m\right)\geq 0\\ H_{\text{upper-level}}\left(y,z_1,\ldots,z_m\right)=0\end{cases}\\
&\qquad\quad z_n \in \arg\max_{z_n} f_{\text{lower-level}}\left(y,z_1,\ldots,z_n,\ldots,z_m\right)\\
&\qquad\qquad \text{s.t:}\begin{cases} g_{\text{lower-level}}\left(y,z_1,\ldots,z_n,\ldots,z_m\right)\geq 0\\ h_{\text{lower-level}}\left(y,z_1,\ldots,z_n,\ldots,z_m\right)=0\end{cases}
\end{aligned} \tag{1}$$

According to Eq. (1), $F_{\text{upper-level}}$ is the leader's objective function, $f_{\text{lower-level}}$ is the follower's objective function, $G_{\text{upper-level}}, H_{\text{upper-level}}, g_{\text{lower-level}}, h_{\text{lower-level}}$ are the leader and follower's unequal and equal constraints, respectively, and $\left(y,z_1,\ldots,z_n,\ldots,z_m\right)$ are decision variables. Based on the above descriptions, when there is more than one decision-maker in the optimization problem, and the win-win game situation is needed to be established among them, the bi-level approach is entirely proper [18]. Figure 2 depicts the schematic of the suggested method. According to this Figure, after implementation of the stochastic programming, the DSO tends to minimize its total operating costs through making a connection with the available independent entity, namely the MGO, trading the energy with the wholesale electricity market, and utilizing its local DERs. On the contrary, the private MGO is inclined to maximize its profit via the same interaction with the DSO, exchanging the energy with the retail electricity market, trading the power with the existing IPL, and finally, using its local DERs. As it is clear, exchanged power and reserve between the DSO and MGO are considered as linking variables of the upper-level and lower-level. Additionally, it should be pointed out that since the optimal day-ahead energy and reserve scheduling is executed from the DSO's perspective, it is chosen as the leader.

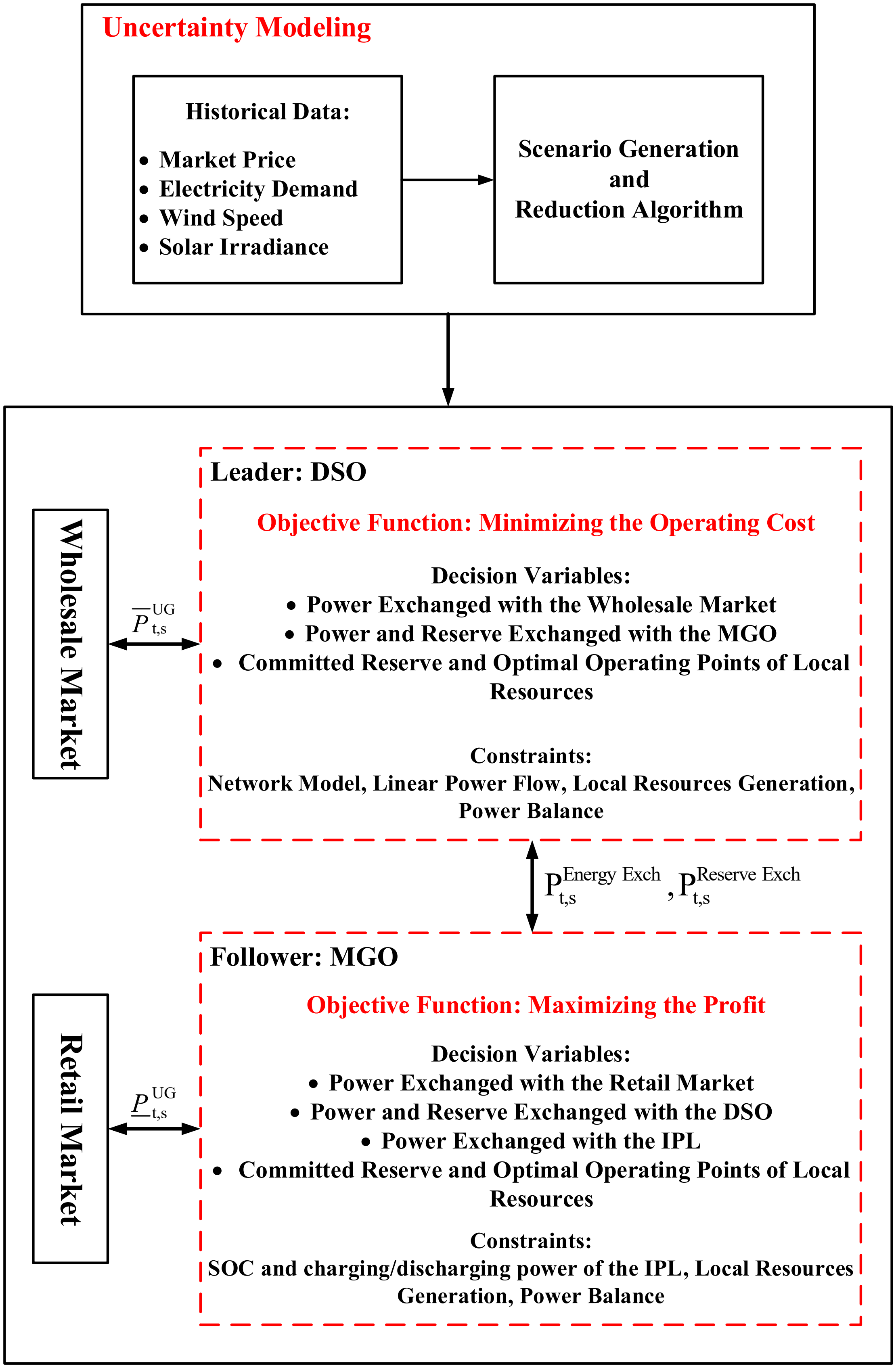

Fig. 2. The proposed Bi-Level decision-making framework.

4. Problem Formulation

As mentioned in the previous part, in this study, the DSO has been considered as the leader of the problem that comprised of several dispatchable units, WTs, PVs, and CAES. While, the private MGO has been considered as the follower of the problem, which is the owner of the environmentally sound IPL, WTs, PVs, and various dispatchable units. These players' objective functions and their operational constraints are formulated in the rest of the paper.

4.1. Objective Function of the Upper-Level: Distribution System Operator

The upper-level's objective function is a single-objective model that minimizes the total operating costs of the DSO which includes the cost of exchanged energy and reserve with the autonomous renewable-based MGO, the cost of exchanged energy with the wholesale market, scheduled power and reserve costs of local dispatchable units, and finally, scheduled power and reserve costs of the local CAES. The decision variables of this level are optimal exchanged power with the wholesale market, optimal exchanged power and reserve with the MGO, optimal operating points, and scheduled reserve by the local DERs.

$$
\begin{aligned}
\mathrm{OF}^{\text{upper-level}} = \min \sum_{t}^{T}\sum_{s}^{S}\pi_{t,s}\Big\{ & \overline{\mathrm{Cost}}_{t,s}^{\mathrm{DG}} + \overline{\mathrm{Cost}}_{t,s}^{\mathrm{CAES}} + \overline{P}_{t,s}^{\mathrm{UG}}\,\overline{\lambda}_{t,s}^{\mathrm{UG}} \\
& + P_{t,s}^{\text{Energy Exch}}\lambda_{t}^{\text{Energy Exch}} + P_{t,s}^{\text{Reserve Exch}}\lambda_{t}^{\text{Reserve Exch}} \\
& + \sum_{\bar{i}}^{\bar{I}} P_{\bar{i},t,s}^{\mathrm{RV,DG}}\,\overline{\lambda}_{\bar{i}}^{\mathrm{RV,DG}} + \sum_{\bar{j}}^{\bar{J}} P_{\bar{j},t,s}^{\mathrm{RV,CAES}}\,\overline{\lambda}_{\bar{j}}^{\mathrm{RV,CAES}} \Big\}
\end{aligned} \tag{2}
$$

4.1.1. Operational Constraints of the Distribution System

In this work, the linear power flow is applied to the studied active distribution network. Eq. (3) calculates the total injected power to the buses.

$$PI^{\mathrm{En}}_{\mathrm{b,t,s}} = \sum_{\mathrm{b'}} PL^{\mathrm{En}}_{\mathrm{b,b',t,s}} = \sum_{\mathrm{b'}} \frac{1}{X_{\mathrm{b,b'}}}\left(\delta^{\mathrm{En}}_{\mathrm{b,t,s}} - \delta^{\mathrm{En}}_{\mathrm{b',t,s}}\right), \qquad \forall_{\mathrm{b,t,s}}$$

$$PI^{\mathrm{Re}}_{\mathrm{b,t,s}} = \sum_{\mathrm{b'}} PL^{\mathrm{Re}}_{\mathrm{b,b',t,s}} = \sum_{\mathrm{b'}} \frac{1}{X_{\mathrm{b,b'}}}\left(\delta^{\mathrm{Re}}_{\mathrm{b,t,s}} - \delta^{\mathrm{Re}}_{\mathrm{b',t,s}}\right), \qquad \forall_{\mathrm{b,t,s}} \tag{3}$$

The power flow between the branches can be calculated and limited by constraints (4) and (5):

$$PL_{\mathrm{b,b',t,s}} = PL^{\mathrm{En}}_{\mathrm{b,b',t,s}} + PL^{\mathrm{Re}}_{\mathrm{b,b',t,s}}, \qquad \forall_{(\mathrm{b,b'})\in\Gamma,\mathrm{t,s}} \tag{4}$$

$$-PL^{\max}_{\mathrm{b,b',t,s}} \le PL_{\mathrm{b,b',t,s}} \le PL^{\max}_{\mathrm{b,b',t,s}}, \qquad \forall_{(\mathrm{b,b'})\in\Gamma,\mathrm{t,s}} \tag{5}$$

Also, the voltage angles are limited by constraint (6):

$$-\pi \le \delta^{\mathrm{En}}_{\mathrm{b,t,s}} \le \pi, \qquad \forall_{\mathrm{b,t,s}}$$

$$-\pi \le \delta^{\mathrm{Re}}_{\mathrm{b,t,s}} \le \pi, \qquad \forall_{\mathrm{b,t,s}} \tag{6}$$

4.1.2. Power Balance of the Distribution System

According to Eq. (7), at each time and each scenario, the power balance of the system should be satisfied.

$$\overline{P}^{\mathrm{UG}}_{\mathrm{b,t,s}} + P^{\mathrm{Energy\ Exch}}_{\mathrm{b,t,s}} + \sum_{\bar{\mathrm{i}}}^{\bar{\mathrm{I}}} P^{\mathrm{DG}}_{\bar{\mathrm{i}},\mathrm{b,t,s}} + \sum_{\bar{\mathrm{k}}}^{\bar{\mathrm{K}}} P^{\mathrm{WT}}_{\bar{\mathrm{k}},\mathrm{b,t,s}} + \sum_{\bar{\mathrm{p}}}^{\bar{\mathrm{P}}} P^{\mathrm{PV}}_{\bar{\mathrm{p}},\mathrm{b,t,s}} + \sum_{\bar{\mathrm{j}}}^{\bar{\mathrm{J}}} P^{\mathrm{cs}}_{\bar{\mathrm{j}},\mathrm{b,t,s}} - \sum_{\bar{\mathrm{j}}}^{\bar{\mathrm{J}}} P^{\mathrm{cp}}_{\bar{\mathrm{j}},\mathrm{b,t,s}} - P^{\mathrm{DSO's\,demand}}_{\mathrm{b,t,s}}$$

$$= PI^{\mathrm{En}}_{\mathrm{b,t,s}}, \qquad \forall_{\mathrm{b,t,s}} \tag{7}$$

4.1.3. Reserve Balance of the Distribution System

In this study, it is assumed that the DSO's local dispatchable units and the CAES are allocated to not only provide the required energy but also compensate for the forecasting errors of renewable resources as well as the load demands. Hence, Eq. (8) imposes the minimum reserve requirements of the considered network.

$$\sum_{\bar{\mathrm{i}}}^{\bar{\mathrm{I}}} P^{\mathrm{RV,DG}}_{\bar{\mathrm{i}},\mathrm{b,t,s}} + \sum_{\bar{\mathrm{j}}}^{\bar{\mathrm{J}}} P^{\mathrm{RV,CAES}}_{\bar{\mathrm{j}},\mathrm{b,t,s}} + P^{\mathrm{Reserve\ Exch}}_{\mathrm{b,t,s}} \ge \overline{\omega}_{\mathrm{wind}} \sum_{\bar{\mathrm{k}}}^{\bar{\mathrm{K}}} P^{\mathrm{WT}}_{\bar{\mathrm{k}},\mathrm{b,t,s}} + \overline{\omega}_{\mathrm{solar}} \sum_{\bar{\mathrm{p}}}^{\bar{\mathrm{P}}} P^{\mathrm{PV}}_{\bar{\mathrm{p}},\mathrm{b,t,s}} + \overline{\omega}_{\mathrm{load}} P^{\mathrm{DSO's\,demand}}_{\mathrm{b,t,s}} + PI^{\mathrm{Re}}_{\mathrm{b,t,s}},$$

$$\forall_{\mathrm{b,t,s}} \tag{8}$$

4.1.4. Constraint of Exchanged Power between the Distribution System Operator and Wholesale Market

Eq. (9) limits the exchanged power between the DSO and the wholesale market:

$$-\overline{P}_{t,s}^{UG,max} \leq \overline{P}_{t,s}^{UG} \leq \overline{P}_{t,s}^{UG,max}, \qquad \forall_{t,s} \tag{9}$$

4.1.5. Constraint of the Upper-Level's Wind Turbine

Eq. (10) is presented to model the produced power of the DSO's WT.

$$P_{\bar{k},t,s}^{WT} = \begin{cases} 0 & , \overline{V}_{t,s} < V_{\bar{k}}^{cut\text{-}in} \text{ or } \overline{V}_{t,s} \geq V_{\bar{k}}^{cut\text{-}out} \\ P_{\bar{k}}^{rated} \dfrac{\overline{V}_{t,s} - V_{\bar{k}}^{cut\text{-}in}}{V_{\bar{k}}^{rated} - V_{\bar{k}}^{cut\text{-}in}} \kappa_{\bar{k}} & , V_{\bar{k}}^{cut\text{-}in} \leq \overline{V}_{t,s} \leq V_{\bar{k}}^{rated} \\ P_{\bar{k}}^{rated} \kappa_{\bar{k}} & , V_{\bar{k}}^{rated} \leq \overline{V}_{t,s} < V_{\bar{k}}^{cut\text{-}out} \end{cases} \tag{10}$$

4.1.6. Constraint of the Upper-Level's Photovoltaic System

The output power of the DSO's PV can be formulated as follows:

$$P_{\bar{p},t,s}^{PV} = \kappa_{\bar{p}} s_{\bar{p}} \eta_{\bar{p}} \overline{G}_{t,s}^{u} \tag{11}$$

4.1.7. Constraints of the Upper-Level's Dispatchable Units

The operating cost of the DSO's dispatchable units can be calculated according to Eq. (12).

$$\overline{\text{Cost}}_{t,s}^{DG} = \sum_{\bar{i}}^{\bar{I}} A_{\bar{i}}^{u} P_{\bar{i},t,s}^{DG} + B_{\bar{i}}^{u} V_{\bar{i},t,s}^{DG} + SUC_{\bar{i},t,s} + SDC_{\bar{i},t,s}, \qquad \forall_{t,s} \tag{12}$$

Eqs. (13) and (14) model the dispatchable units' startup and shutdown costs.

$$SUC_{\bar{i},t,s} \geq \overline{S}_{\bar{i}}^{uc} (V_{\bar{i},t,s}^{DG} - V_{\bar{i},t-1,s}^{DG}), \qquad \forall_{\bar{i},t,s} \tag{13}$$

$$SDC_{\bar{i},t,s} \geq \overline{S}_{\bar{i}}^{dc} (V_{\bar{i},t-1,s}^{DG} - V_{\bar{i},t,s}^{DG}), \qquad \forall_{\bar{i},t,s} \tag{14}$$

The dispatchable units' maximum and minimum limits are represented in Eqs. (15) and (16) [34].

$$P_{\bar{i},t,s}^{DG} \geq \overline{P}_{\bar{i}}^{min} V_{\bar{i},t,s}^{DG}, \qquad \forall_{\bar{i},t,s} \tag{15}$$

$$P_{\bar{i},t,s}^{DG} + P_{\bar{i},t,s}^{RV,DG} \leq \overline{P}_{\bar{i}}^{max} V_{\bar{i},t,s}^{DG}, \qquad \forall_{\bar{i},t,s} \tag{16}$$

The dispatchable units' ramp-up and ramp-down rate constraints are provided in Eqs. (17) and (18) [35].

$$P_{\bar{i},t,s}^{DG} - P_{\bar{i},t-1,s}^{DG} \leq RU_{\bar{i}}^{U} V_{\bar{i},t,s}^{DG}, \qquad \forall_{\bar{i},t,s} \tag{17}$$

$$P_{\bar{i},t-1,s}^{DG} - P_{\bar{i},t,s}^{DG} \leq RD_{\bar{i}}^{U} V_{\bar{i},t-1,s}^{DG}, \qquad \forall_{\bar{i},t,s} \tag{18}$$

The minimum on/off time and minimum up/down-time constraints of dispatchable units are shown in Eqs. (19)-(22).

$$V_{\bar{i},t,s}^{DG} - V_{\bar{i},t-1,s}^{DG} \leq V_{\bar{i},t+TU_{\bar{i},\bar{n}},s}^{DG}, \qquad \forall_{\bar{i},t,s} \tag{19}$$

$$V_{\bar{i},t-1,s}^{DG} - V_{\bar{i},t,s}^{DG} \leq 1 - V_{\bar{i},t+TD_{\bar{i},\bar{n}},s}^{DG}, \qquad \forall_{\bar{i},t,s} \tag{20}$$

$$TU_{\bar{i},\bar{n}} = \begin{cases} \bar{n} & \bar{n} \leq MUT_{\bar{i}} \\ 0 & \bar{n} > MUT_{\bar{i}} \end{cases}, \qquad \forall_{\bar{i}} \tag{21}$$

$$TD_{\bar{i},\bar{n}} = \begin{cases} \bar{n} & \bar{n} \leq MDT_{\bar{i}} \\ 0 & \bar{n} > MDT_{\bar{i}} \end{cases}, \qquad \forall_{\bar{i}} \tag{22}$$

Finally, the available capacity of dispatchable units for reserve requirements can be formulated as Eq. (23).

$$0 \leq P_{\bar{i},t,s}^{RV,DG} \leq \psi \overline{P}_{\bar{i}}^{max}, \qquad \forall_{\bar{i},t,s} \tag{23}$$

4.1.8. Constraints of the Upper-Level's Compressed Air Energy Storage system

The operating cost of the DSO's CAES unit is expressed in Eq. (24) [36].

$$\overline{Cost}_{t,s}^{CAES} = \sum_{\bar{j}}^{\bar{J}} \left[P_{\bar{j},t,s}^{cp} vom_{\bar{j}}^{inj} \right] + \left[P_{\bar{j},t,s}^{cs} \left(HR_{\bar{j}}^{p} \lambda_{g} + vom_{\bar{j}}^{p} \right) \right], \qquad \forall_{t,s} \tag{24}$$

Injected air into the system can be formulated by Eq. (25).

$$V_{\bar{j},t,s}^{inj} = b_{\bar{j}}^{inj} P_{\bar{j},t,s}^{cp}, \qquad \forall_{\bar{j},t,s} \tag{25}$$

Eq. (26) illustrates the amount of provided energy and reserve by the CAES system.

$$P_{\bar{j},t,s}^{cs} + P_{\bar{j},t,s}^{RV,CAES} = b_{\bar{j}}^{p} V_{\bar{j},t,s}^{p}, \qquad \forall_{\bar{j},t,s} \tag{26}$$

Eqs. (27) and (28) present the mathematical model for the stored air in the storage and pumped air from the CAES into the combustion chamber, respectively.

$$V_{j}^{inj,min} U_{j,t,s}^{inj} \le V_{j,t,s}^{inj} \le V_{j}^{inj,max} U_{j,t,s}^{inj}, \qquad \forall_{j,t,s} \tag{27}$$

$$V_{j}^{p,min} U_{j,t,s}^{p} \le V_{j,t,s}^{p} \le V_{j}^{p,max} U_{j,t,s}^{p}, \qquad \forall_{j,t,s} \tag{28}$$

Eq. (29) prevents the CAES from the simultaneous store and pumping performances.

$$U_{j,t,s}^{p} + U_{j,t,s}^{inj} \le 1, \qquad \forall_{j,t,s} \tag{29}$$

Ultimately, the amount of stored energy in the CAES and its limitations are represented in Eqs. (30) and (31).

$$SOC_{j,t,s}^{CAES} = SOC_{j,t-1,s}^{CAES} + V_{j,t,s}^{inj} - V_{j,t,s}^{p}, \qquad \forall_{j,t,s} \tag{30}$$

$$SOC_{j,t,s}^{CAES,min} \le SOC_{j,t,s}^{CAES} \le SOC_{j,t,s}^{CAES,max}, \qquad \forall_{j,t,s} \tag{31}$$

4.2. Objective Function of the Lower-Level: Microgrid Owner

The objective function of this level is the maximization of the autonomous MGO's profit that can be defined as the difference between its incomes and expenses. The MGO's revenue includes the cost of exchanged energy and reserve with the DSO, the cost of exchanged energy with the retail market, and the cost of selling power to the local IPL. On the other hand, the MGO's expenses consist of the cost of providing energy and reserve from the local IPL, and scheduled power and reserve costs of the local dispatchable units. The decision variables of this level are optimal exchanged power with the retail market, optimal exchanged power and reserve with the DSO, optimal exchanged power with the IPL, and finally, committed reserve and operating points of the local DERs.

$$\text{OF}^{\text{lower-level}} = \max \sum_{t}^{T} \sum_{s}^{S} \pi_{t,s} \Big\{ P_{t,s}^{\text{Energy Exch}} \lambda_{t}^{\text{Energy Exch}} + P_{t,s}^{\text{Reserve Exch}} \lambda_{t}^{\text{Reserve Exch}} + \underline{P}_{t,s}^{\text{UG}} \underline{\lambda}_{t,s}^{\text{UG}} + \sum_{\underline{j}}^{J} P_{\underline{j},t,s}^{\text{Ch,EV}} \underline{\lambda}_{\underline{j}}^{\text{Ch,EV}} - \underline{\text{Cost}}_{t,s}^{\text{DG}} - \sum_{\underline{i}}^{I} P_{\underline{i},t,s}^{\text{RV,DG}} \underline{\lambda}_{\underline{i}}^{\text{RV,DG}} - \sum_{\underline{j}}^{J} P_{\underline{j},t,s}^{\text{Dch,EV}} \underline{\lambda}_{\underline{j}}^{\text{Dch,EV}} - \sum_{\underline{j}}^{J} P_{\underline{j},t,s}^{\text{RV,EV}} \underline{\lambda}_{\underline{j}}^{\text{RV,EV}} \Big\} \tag{32}$$

4.2.1. Power Balance of the Microgrid

The MGO's local demands have to be equal to the sum of the exchanged power with the DSO, retail market, IPL, and produced power by the DERs.

$$\underline{P}_{t,s}^{\text{UG}} + \sum_{\underline{i}}^{I} P_{\underline{i},t,s}^{\text{DG}} + \sum_{\underline{k}}^{K} P_{\underline{k},t,s}^{\text{WT}} + \sum_{\underline{p}}^{P} P_{\underline{p},t,s}^{\text{PV}} + \sum_{\underline{j}}^{J} P_{\underline{j},t,s}^{\text{Dch,EV}} = P_{t,s}^{\text{Energy Exch}} + \sum_{\underline{j}}^{J} P_{\underline{j},t,s}^{\text{Ch,EV}} + P_{t,s}^{\text{MGO's demand}} \quad \forall_{t,s} \quad \lambda_{t,s}^{1} \tag{33}$$

4.2.2. Reserve Balance of the Microgrid

Similar to the upper-level, the MGO's IPL and local dispatchable units are considered to not only provide the system's required energy but also compensate for the forecasting errors of renewable resources and the load demands. Eq. (34) expresses the lower-level's reserve constraint.

$$\sum_{\underline{i}}^{I} P_{\underline{i},t,s}^{\text{RV,DG}} + \sum_{\underline{j}}^{J} P_{\underline{j},t,s}^{\text{RV,EV}} \geq P_{t,s}^{\text{Reserve Exch}} + \underline{\omega}_{\text{wind}} \sum_{\underline{k}}^{K} P_{\underline{k},t,s}^{\text{WT}} + \underline{\omega}_{\text{solar}} \sum_{\underline{p}}^{P} P_{\underline{p},t,s}^{\text{PV}} + \underline{\omega}_{\text{load}} P_{t,s}^{\text{MGO's demand}} \quad \forall_{t,s} \quad \mu_{t,s}^{1} \tag{34}$$

4.2.3. Constraints of the Contracted Exchanged Power and Reserve between the Microgrid and Distribution System Operator

Eqs. (35) and (36) demonstrate the possible exchanged power and reserve between the DSO and MGO.

$$-P_{t,s}^{\text{Energy Exch,max}} \leq P_{t,s}^{\text{Energy Exch}} \leq P_{t,s}^{\text{Energy Exch,max}}, \quad \forall_{t,s} \quad \mu_{t,s}^{2}, \mu_{t,s}^{3} \tag{35}$$

$$-P_{t,s}^{\text{Reserve Exch,max}} \le P_{t,s}^{\text{Reserve Exch}} \le P_{t,s}^{\text{Reserve Exch,max}}, \qquad \forall_{t,s} \quad \mu_{t,s}^{4}, \mu_{t,s}^{5} \tag{36}$$

4.2.4. Constraint of the Exchanged Power between the Microgrid and Retail Market

The exchanged power between the MGO and the retail market can be limited by Eq. (37).

$$-\underline{P}_{t,s}^{\text{UG,max}} \le \underline{P}_{t,s}^{\text{UG}} \le \underline{P}_{t,s}^{\text{UG,max}}, \qquad \forall_{t,s} \quad \mu_{t,s}^{6}, \mu_{t,s}^{7} \tag{37}$$

4.2.5. Constraint of the Lower-Level's Wind Turbine

The output power of the MGO's WT can be defined as follows:

$$P_{\underline{k},t,s}^{\text{WT}} = \begin{cases} 0 & , \underline{V}_{t,s} < V_{\underline{k}}^{\text{cut-in}} \text{ or } \underline{V}_{t,s} \ge V_{\underline{k}}^{\text{cut-out}} \\ P_{\underline{k}}^{\text{rated}} \dfrac{\underline{V}_{t,s} - V_{\underline{k}}^{\text{cut-in}}}{V_{\underline{k}}^{\text{rated}} - V_{\underline{k}}^{cut-in}} \kappa_{\underline{k}} & , V_{\underline{k}}^{\text{cut-in}} \le \underline{V}_{t,s} \le V_{\underline{k}}^{\text{rated}} \\ P_{\underline{k}}^{\text{rated}} \kappa_{\underline{k}} & , V_{\underline{k}}^{\text{rated}} \le \underline{V}_{t,s} < V_{\text{k\_}}^{\text{cut-out}} \end{cases} \tag{38}$$

4.2.6. Constraint of the Lower-Level's Photovoltaic System

The output power of the MGO's PV is calculated by Eq. (39).

$$P_{\underline{p},t,s}^{\text{PV}} = \kappa_{\underline{p}} s_{\underline{p}} \eta_{\underline{p}} \underline{G}_{t,s}^{1} \tag{39}$$

4.2.7. Constraints of the Lower-Level's Dispatchable Units

The following equations model the operating cost and startup cost of the MGO's dispatchable units.

$$\underline{\text{Cost}}_{t,s}^{\text{DG}} = \sum_{\underline{i}}^{\text{I}} B_{\underline{i}}^{1} P_{\underline{i},t,s}^{\text{DG}} + SUC_{\underline{i},t,s}, \qquad \forall_{t,s} \tag{40}$$

$$SUC_{\underline{i},t,s} \ge \underline{S}_{\underline{i}}^{\text{uc}} (V_{\underline{i},t,s}^{\text{DG}} - V_{\underline{i},t-1,s}^{\text{DG}}), \qquad \forall_{\underline{i},t,s} \tag{41}$$

Eqs. (42), (43) model the operation limits of the dispatchable units.

$$P_{\underline{i},t,s}^{\text{DG}} \ge V_{\underline{i},t,s}^{\text{DG}} \underline{P}_{\underline{i}}^{\min}, \qquad \forall_{\underline{i},t,s} \quad \mu_{\underline{i},t,s}^{8} \tag{42}$$

$$P_{\underline{i},t,s}^{\text{DG}} + P_{\underline{i},t,s}^{\text{RV,DG}} \le V_{\underline{i},t,s}^{\text{DG}} \underline{P}_{\underline{i}}^{\max}, \qquad \forall_{\underline{i},t,s} \quad \mu_{\underline{i},t,s}^{9} \tag{43}$$

The ramp-up and ramp-down rate constraints of the dispatchable units can be formulated as follows:

$$P_{i,t,s}^{DG} - P_{i,t-1,s}^{DG} \le RU_i^L V_{i,t,s}^{DG}, \qquad \forall_{i,t,s} \quad \mu_{i,t,s}^{10} \tag{44}$$

$$P_{i,t-1,s}^{DG} - P_{i,t,s}^{DG} \le RD_i^L V_{i,t-1,s}^{DG}, \qquad \forall_{i,t,s} \quad \mu_{i,t,s}^{11} \tag{45}$$

Ultimately, the available capacity of dispatchable units for reserve requirements is formulated as Eq. (46).

$$0 \le P_{i,t,s}^{RV,DG} \le \psi \underline{P}_i^{max}, \qquad \forall_{i,t,s} \quad \mu_{i,t,s}^{12}, \mu_{i,t,s}^{13} \tag{46}$$

4.2.8. Constraints of the Lower-Level's Intelligent Parking Lot

Eqs. (47)-(48) indicate the charge/discharge limitation of each EV. Also, inequality (49) is used to avoid the simultaneous charge and discharge of the EVs.

$$P_{j,t,s}^{Ch,EV} \le P_j^{Ch,max} W_{j,t,s}^{Ch} M_{j,t}, \qquad \forall_{j,t,s} \quad \mu_{j,t,s}^{14} \tag{47}$$

$$P_{j,t,s}^{Dch,EV} + P_{j,t,s}^{RV,EV} \le P_j^{Dch,max} W_{j,t,s}^{Dch} M_{j,t}, \qquad \forall_{j,t,s} \quad \mu_{j,t,s}^{15} \tag{48}$$

$$W_{j,t,s}^{Ch} + W_{j,t,s}^{Dch} \le M_{j,t}, \qquad \forall_{j,t,s} \tag{49}$$

Based on the EVs' battery life, Eq. (50) limits the number of switching between the charge and discharge status of the existed EVs in the IPL.

$$\sum_{t=t^{min}}^{t^{max}} W_{j,t,s}^{ch} + W_{j,t,s}^{dch} \le N^{max}, \qquad \forall_{j,s} \tag{50}$$

The scheduled reserve by the existed EVs in the IPL is formulated as follows:

$$P_{j,t,s}^{RV,EV} \le \sigma P_j^{Dch,max} SRS_{j,t,s} M_{j,t}, \qquad \forall_{j,t,s} \quad \mu_{j,t,s}^{16} \tag{51}$$

$$P_{j,t,s}^{RV,EV} \le \sigma P_j^{Dch,max} W_{j,t,s}^{Dch} M_{j,t}, \qquad \forall_{j,t,s} \quad \mu_{j,t,s}^{17} \tag{52}$$

Constraints (53) and (54) are utilized to model and limit the EVs' state of charge.

$$SOC_{j,t,s}^{IPL} = SOC_{j,t-1,s}^{IPL} + P_{j,t,s}^{Ch,EV} \eta^{g2v} - (P_{j,t,s}^{Dch,EV} + P_{j,t,s}^{RV,EV}) / \eta^{v2g}, \qquad \forall_{j,t,s} \quad \lambda_{j,t,s}^{2} \tag{53}$$

$$SOC_j^{IPL,min} \le SOC_{j,t,s}^{IPL} \le SOC_j^{IPL,max}, \qquad \forall_{j,t,s} \quad \mu_{j,t,s}^{18}, \mu_{j,t,s}^{19} \tag{54}$$

Some batteries of EVs are charged too fast and vice versa. Thus, constraint (55) is considered to limit the maximum charge and discharge rates of the EVs.

$$-\Delta SOC_{j}^{\max} \leq SOC_{j,t,s}^{\text{IPL}} - SOC_{j,t-1,s}^{\text{IPL}} \leq \Delta SOC_{j}^{\max}, \qquad \forall_{j,t,s} \quad \mu_{j,t,s}^{20}, \mu_{j,t,s}^{21} \tag{55}$$

The EVs' state of charge should be equal or higher than a specific level at the departure time from the IPL. Therefore, Eq. (56) is provided to satisfy the mentioned situation. It should be noted that the EV owners determine the level of the limitation. Finally, inequality (57) determines the EVs' state of charge at the arrival time to the IPL.

$$SOC_{j,t,s}^{\text{IPL}} \geq \chi SOC_{j}^{\text{IPL,max}}, \qquad \forall_{j,t^{\text{Dep.}},s} \quad \mu_{j,t^{\text{Dep.}},s}^{22} \tag{56}$$

$$SOC_{j,t,s}^{\text{IPL}} \geq SOC_{j}^{\text{Arrival}}, \qquad \forall_{j,t^{\text{Arv.}},s} \quad \mu_{j,t^{\text{Arv.}},s}^{23} \tag{57}$$

5. Reformulation of the Bi-Level as a Mathematical Program with Equilibrium Constraints

Generally, there are varied methods to solve the bi-level optimization problems, two of which are Karush-Kuhn-Tucker (KKT) and Primal-Dual formulations [37]. It is noteworthy that the KKT technique is the typical approach, in which the lower-level of the problem is substituted with its KKT conditions. However, it should be considered that the lower-level of the optimization problem can be replaced with its KKT conditions if it is linear [38]. Subsequently, by utilizing the KKT formulations, the non-linear bi-level model is transformed into a non-linear single-level model. The non-linearity of this approach results from its complementary constraints [39]. As a result, in this article, the Big-M method is exploited to make these kinds of constraints linear. The detailed mathematical formulation of the applied method is provided in Ref. [40]. According to the provided explanation and the presented references, the final linear single-level model of the studied bi-level stochastic programming problem is formulated as follows:

$$\underset{\substack{P^{\text{Energy Exch}}_{t,s}\ \overline{P}^{\text{UG}}_{t,s}\ P^{\text{DG}}_{\bar{i},t,s}\ P^{\text{RV,DG}}_{\bar{i},t,s}\ P^{\text{cp}}_{\bar{j},t,s}\ P^{\text{Ch,EV}}_{\underline{j},t,s}\ P^{\text{RV,CAES}}_{\bar{j},t,s} \\ P^{\text{Reserve Exch}}_{t,s}\ \underline{P}^{\text{UG}}_{t,s}\ P^{\text{DG}}_{\underline{i},t,s}\ P^{\text{RV,DG}}_{\underline{i},t,s}\ P^{\text{cs}}_{\bar{j},t,s}\ P^{\text{Dch,EV}}_{\underline{j},t,s}\ P^{\text{RV,EV}}_{\underline{j},t,s}}}{\text{Min}}\ \text{OF}^{\text{single-level}}$$

$$\sum_{t}^{T}\sum_{s}^{S}\pi_{t,s}\Bigg\{\overline{\text{Cost}}^{\text{DG}}_{t,s}+\overline{\text{Cost}}^{\text{CAES}}_{t,s}+\overline{P}^{\text{UG}}_{t,s}\,\overline{\lambda}^{\text{UG}}_{t,s} + P^{\text{Energy Exch}}_{t,s}\lambda^{\text{Energy Exch}}_{t}+P^{\text{Reserve Exch}}_{t,s}\lambda^{\text{Reserve Exch}}_{t} + \sum_{\bar{i}}^{\bar{I}}P^{\text{RV,DG}}_{\bar{i},t,s}\overline{\lambda}^{\text{RV,DG}}_{\bar{i}}+\sum_{\bar{j}}^{\bar{J}}P^{\text{RV,CAES}}_{\bar{j},t,s}\overline{\lambda}^{\text{RV,CAES}}_{\bar{j}}\Bigg\} \tag{58}$$

Subject-to:

Equations: (3)-(31), (33), (38)-(41), (49)-(50), (53) (59)

- Stationary Constraints:

$$\pi_{t,s}\lambda^{\text{Energy Exch}}_{t}-\lambda^{1}_{t,s}+\mu^{2}_{t,s}-\mu^{3}_{t,s}=0 \tag{60}$$

$$\pi_{t,s}\lambda^{\text{Reserve Exch}}_{t}-\mu^{1}_{t,s}+\mu^{4}_{t,s}-\mu^{5}_{t,s}=0 \tag{61}$$

$$\pi_{t,s}\underline{\lambda}^{\text{UG}}_{t,s}+\lambda^{1}_{t,s}+\mu^{6}_{t,s}-\mu^{7}_{t,s}=0 \tag{62}$$

$$\pi_{t,s}\underline{\lambda}^{\text{Ch,EV}}_{\underline{j}}-\lambda^{1}_{t,s}-\mu^{14}_{\underline{j},t,s}-\lambda^{2}_{\underline{j},t,s}\eta^{\text{g2v}}=0 \tag{63}$$

$$-\pi_{t,s}\underline{\lambda}^{\text{Dch,EV}}_{\underline{j}}+\lambda^{1}_{t,s}-\mu^{15}_{\underline{j},t,s}+\lambda^{2}_{\underline{j},t,s}/\eta^{\text{v2g}}=0 \tag{64}$$

$$-\pi_{t,s}\underline{\lambda}^{\text{RV,EV}}_{\underline{j}}+\mu^{1}_{t,s}-\mu^{15}_{\underline{j},t,s}-\mu^{16}_{\underline{j},t,s}-\mu^{17}_{\underline{j},t,s}+\lambda^{2}_{\underline{j},t,s}/\eta^{\text{v2g}}=0 \tag{65}$$

$$-\pi_{t,s}B^{1}_{\underline{i}}+\lambda^{1}_{t,s}+\mu^{8}_{\underline{i},t,s}-\mu^{9}_{\underline{i},t,s}-\mu^{10}_{\underline{i},t,s}+\mu^{11}_{\underline{i},t,s}=0 \tag{66}$$

$$-\pi_{t,s}\underline{\lambda}^{\text{RV,DG}}_{\underline{i}}+\mu^{1}_{t,s}-\mu^{9}_{\underline{i},t,s}+\mu^{12}_{\underline{i},t,s}-\mu^{13}_{\underline{i},t,s}=0 \tag{67}$$

- Primal, Dual, and Complementary Constraints:

$$0\le\left[\begin{array}{l}\sum_{\underline{i}}^{\underline{I}}P^{\text{RV,DG}}_{\underline{i},t,s}+\sum_{\underline{j}}^{\underline{J}}P^{\text{RV,EV}}_{\underline{j},t,s}-P^{\text{Reserve Exch}}_{t,s} \\ -\underline{\omega}_{\text{wind}}\sum_{\underline{k}}^{\underline{K}}P^{\text{WT}}_{\underline{k},t,s}-\underline{\omega}_{\text{solar}}\sum_{\underline{p}}^{\underline{P}}P^{\text{PV}}_{\underline{p},t,s}-\underline{\omega}_{\text{load}}P^{\text{MGO's demand}}_{t,s}\end{array}\right]\perp\mu^{1}_{t,s}\ge0 \tag{68}$$

$$0\le P^{\text{Energy Exch}}_{t,s}+P^{\text{Energy Exch,max}}_{t,s}\perp\mu^{2}_{t,s}\ge0 \tag{69}$$

$$0\le P^{\text{Energy Exch,max}}_{t,s}-P^{\text{Energy Exch}}_{t,s}\perp\mu^{3}_{t,s}\ge0 \tag{70}$$

$$0\le P^{\text{Reserve Exch}}_{t,s}+P^{\text{Reserve Exch,max}}_{t,s}\perp\mu^{4}_{t,s}\ge0 \tag{71}$$

$$0\le P^{\text{Reserve Exch,max}}_{t,s}-P^{\text{Reserve Exch}}_{t,s}\perp\mu^{5}_{t,s}\ge0 \tag{72}$$

$$0 \le \underline{P}_{t,s}^{UG} + \underline{P}_{t,s}^{UG,max} \perp \mu_{t,s}^{6} \ge 0 \quad (73)$$

$$0 \le \underline{P}_{t,s}^{UG,max} - \underline{P}_{t,s}^{UG} \perp \mu_{t,s}^{7} \ge 0 \quad (74)$$

$$0 \le P_{i,t,s}^{DG} - V_{i,t,s}^{DG} \underline{P}_{i}^{min} \perp \mu_{i,t,s}^{8} \ge 0 \quad (75)$$

$$0 \le V_{i,t,s}^{DG} \underline{P}_{i}^{max} - P_{i,t,s}^{DG} - P_{i,t,s}^{RV,DG} \perp \mu_{i,t,s}^{9} \ge 0 \quad (76)$$

$$0 \le RU_{i}^{L} V_{i,t,s}^{DG} - P_{i,t,s}^{DG} + P_{i,t-1,s}^{DG} \perp \mu_{i,t,s}^{10} \ge 0 \quad (77)$$

$$0 \le RD_{i}^{L} V_{i,t-1,s}^{DG} - P_{i,t-1,s}^{DG} + P_{i,t,s}^{DG} \perp \mu_{i,t,s}^{11} \ge 0 \quad (78)$$

$$0 \le P_{i,t,s}^{RV,DG} \perp \mu_{i,t,s}^{12} \ge 0 \quad (79)$$

$$0 \le \psi \underline{P}_{i}^{max} - P_{i,t,s}^{RV,DG} \perp \mu_{i,t,s}^{13} \ge 0 \quad (80)$$

$$0 \le P_{j}^{Ch,max} W_{j,t,s}^{Ch} M_{j,t} - P_{j,t,s}^{Ch,EV} \perp \mu_{j,t,s}^{14} \ge 0 \quad (81)$$

$$0 \le P_{j}^{Dch,max} W_{j,t,s}^{Dch} M_{j,t} - P_{j,t,s}^{Dch,EV} - P_{j,t,s}^{RV,EV} \perp \mu_{j,t,s}^{15} \ge 0 \quad (82)$$

$$0 \le \sigma P_{j}^{Dch,max} SRS_{j,t,s} M_{j,t} - P_{j,t,s}^{RV,EV} \perp \mu_{j,t,s}^{16} \ge 0 \quad (83)$$

$$0 \le \sigma P_{j}^{Dch,max} W_{j,t,s}^{Dch} M_{j,t} - P_{j,t,s}^{RV,EV} \perp \mu_{j,t,s}^{17} \ge 0 \quad (84)$$

$$0 \le SOC_{j,t,s}^{IPL} - SOC_{j}^{IPL,min} \perp \mu_{j,t,s}^{18} \ge 0 \quad (85)$$

$$0 \le SOC_{j}^{IPL,max} - SOC_{j,t,s}^{IPL} \perp \mu_{j,t,s}^{19} \ge 0 \quad (86)$$

$$0 \le SOC_{j,t,s}^{IPL} - SOC_{j,t-1,s}^{IPL} + \Delta SOC_{j}^{max} \perp \mu_{j,t,s}^{20} \ge 0 \quad (87)$$

$$0 \le \Delta SOC_{j}^{max} - SOC_{j,t,s}^{IPL} + SOC_{j,t-1,s}^{IPL} \perp \mu_{j,t,s}^{21} \ge 0 \quad (88)$$

$$0 \le SOC_{j,t,s}^{IPL} - \chi SOC_{j}^{IPL,max} \perp \mu_{j,t^{Dep},s}^{22} \ge 0 \quad (89)$$

$$0 \le SOC_{j,t,s}^{IPL} - SOC_{j}^{Arrival} \perp \mu_{j,t^{Arv.},s}^{23} \ge 0 \quad (90)$$

$$\lambda_{t,s}^{1}, \lambda_{j,t,s}^{2} \quad \text{Unrestricted} \quad (91)$$

- The linear form of Complementary Constraints:

Each complementary constraint as provided in Eqs. (68)-(90) is linearized as (92), in which X is a binary variable, and M is a sufficiently large value.

$$0 \le \alpha \perp \beta \ge 0 \rightarrow \alpha \ge 0, \beta \ge 0 \rightarrow \begin{cases} \alpha \le \mathrm{MX} \\ \beta \le \mathrm{M}(1-\mathrm{X}) \end{cases} \quad (92)$$

6. Numerical Simulation

The suggested bi-level optimization model comprised of the DSO and an independent ecologically sound MGO that are collaborated. In other words, the DSO is considered as the leader of the problem, which is the owner of six different dispatchable units, and eco-friendly units such as WTs, PVs, and CAES. On the other hand, the independent MGO is considered as the follower of the problem, which is the owner of three different dispatchable units, and ozone-friendly units such as the IPL, WTs, and PVs. Minimizing the total operating costs of the DSO, as well as maximizing the expected profit of the renewable-based MGO is the primary purpose of this paper. The proposed problem is analyzed in four different case studies, with and without considering the eco-efficient units, CAES, and IPL, that play a significant role in the optimal performance of the studied system. The classification of the mentioned case studies is presented in Table 3.

Table 3: Classification of four case studies in the paper.

	Compressed Air Energy Storage	Intelligent Parking Lot
Case Study 1	✗	✗
Case Study 2	✓	✗
Case Study 3	✗	✓
Case Study 4	✓	✓

The proposed method is applied to the modified IEEE 15-Bus ADS, as shown in Figure 3. The DSO's local DERs are located at Buses 7, 8, 10, 11, 13, and 15. Also, it is assumed that the DSO exchanges the energy and reserve with the MGO through the Bus 14.

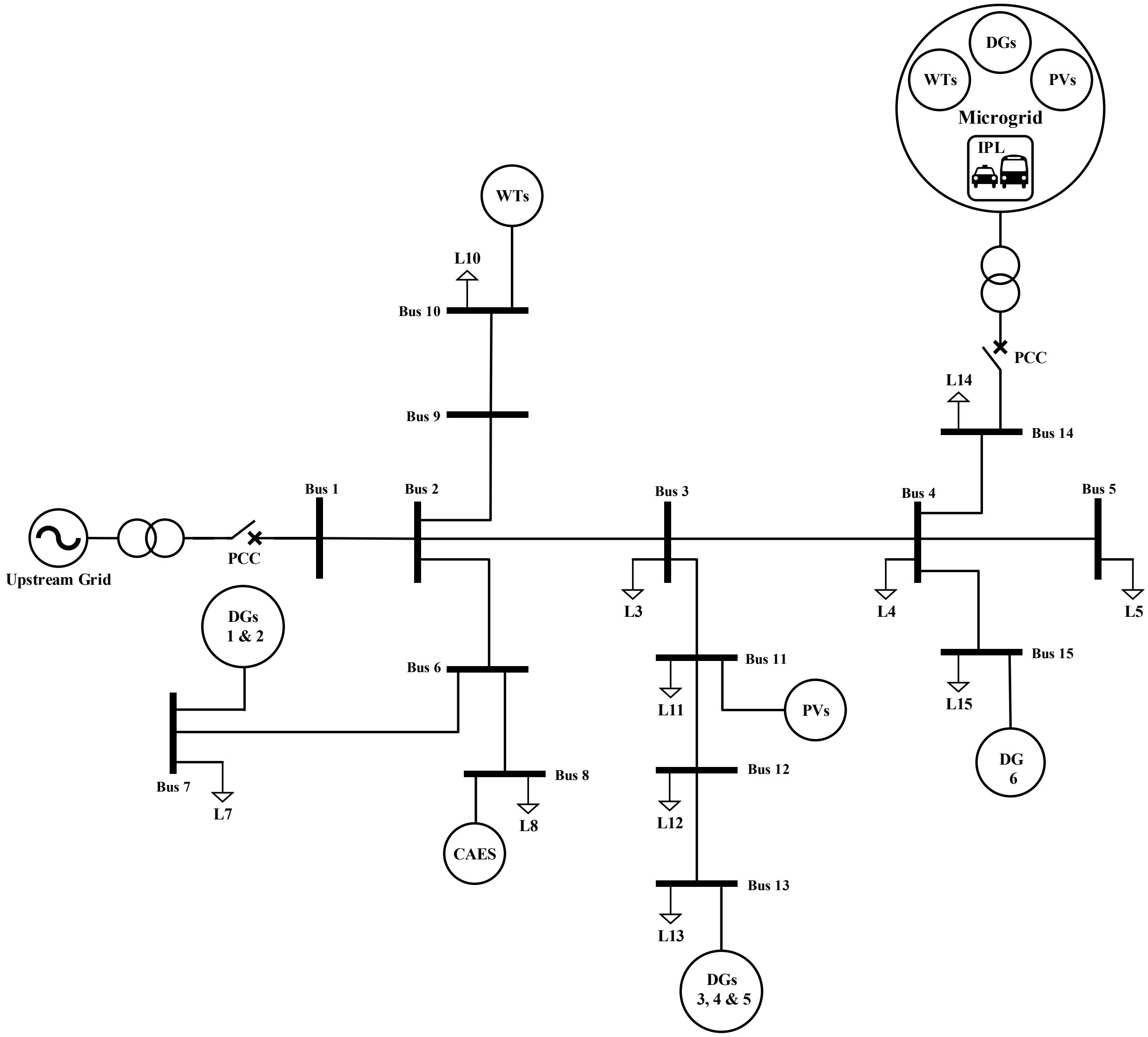

Fig. 3. One-line diagram of the modified IEEE 15-Bus network.

6.1. Input Data

Input data of the DSO and MGO's dispatchable units are listed in Table 4.

Table 4: Data of the upper/lower-level's dispatchable units.

The upper level's dispatchable units							
Units	$\overline{P}_i^{min}$	$\overline{P}_i^{max}$	A_i^u	B_i^u	$\overline{S}_i^{uc} / \overline{S}_i^{dc}$	RU_i^U / RD_i^U	MUT_i / MDT_i
	MW	MW	\$/MWh	\$/h	\$	MW/h	h
1	0.1	2.0	45.2	31.6	32 / 0	0.5 / 0.5	1
2	0.1	2.5	48.2	41.6	38 / 0	0.5 / 0.5	1
3	0.1	1.0	46.2	51.6	30 / 0	0.5 / 0.5	1
4	0.2	2.5	72.8	16.7	52 / 0	1.0 / 1.0	3
5	0.3	3.0	62.8	26.7	55 / 0	1.5 / 1.5	3
6	0.1	1.5	46.2	34.6	35 / 0	0.5 / 0.5	1
The lower level's dispatchable units							

Unit	$\underline{P}_{\underline{i}}^{min}$	$\underline{P}_{\underline{i}}^{max}$	$B_{\underline{i}}^{l}$	$S_{\underline{i}}^{uc}$	$RU_{\underline{i}}^{L}$	$RD_{\underline{i}}^{L}$
	MW	MW	\$/MWh	\$	MW/h	MW/h
1	0.15	0.95	56	30	0.35	0.35
2	0.10	0.90	51	25	0.20	0.20
3	0.05	0.85	47	20	0.15	0.15

The input data of the PVs, WTs, CAES, and IPL are stated in Table 5 [30, 31]. It is noted that the capacity of the ecologically sound IPL is 230 EVs. Also, the EV owners park their car between 2~8 hours in the parking lot [31].

Table 5: PVs, WTs, CAES, and IPL data.

Parameter	Unit	Value	Parameter	Unit	Value
The upper level's PV					
$\eta_{\bar{p}}$	%	14	$\kappa_{\bar{p}}$	Constant	30
$s_{\bar{p}}$	m^2	500			
The lower level's PV					
$\eta_{\underline{p}}$	%	14	$\kappa_{\underline{p}}$	Constant	21
$s_{\underline{p}}$	m^2	200			
The upper level's WT					
$P_{\bar{k}}^{rated}$	MW	2.05	$V_{\bar{k}}^{cut\text{-}in}$	m/s	5
$V_{\bar{k}}^{rated}$	m/s	14	$V_{\bar{k}}^{cut\text{-}out}$	m/s	25
$\kappa_{\bar{k}}$	Constant	3			
The lower level's WT					
$P_{\underline{k}}^{rated}$	kW	49.9	$V_{\underline{k}}^{cut\text{-}in}$	m/s	2.5
$V_{\underline{k}}^{rated}$	m/s	8.5	$V_{\underline{k}}^{cut\text{-}out}$	m/s	25
$\kappa_{\underline{k}}$	Constant	20			
The upper-level's CAES					
$SOC_{\bar{j},t,s}^{CAES,min}$	MWh	0.4	$SOC_{\bar{j},t,s}^{CAES,max}$	MWh	4
$V_{\bar{j}}^{inj,min}$	MWh	0.1	$V_{\bar{j}}^{inj,max}$	MWh	0.5
$V_{\bar{j}}^{p,min}$	MWh	0.1	$V_{\bar{j}}^{p,max}$	MWh	0.5
$b_{\bar{j}}^{inj}$	%	95	$b_{\bar{j}}^{p}$	%	95
$vom_{\bar{j}}^{inj}$	\$/MWh	3.095	$vom_{\bar{j}}^{p}$	\$/MWh	3.095
$HR_{\bar{j}}^{p}$	MMBtu/MWh	3.9998	λ_g	\$/MMBtu	1.87
The lower-level's IPL					
$\lambda_{\underline{j}}^{Ch,EV}$	\$/kWh	0.25~0.40	$\lambda_{\underline{j}}^{Dch,EV}$	\$/kWh	0.15~0.35

$SOC_{j,t,s}^{IPL,min}$	kWh	0	$SOC_{j,t,s}^{IPL,max}$	kWh	10~20
$SOC_{j}^{Arrival}$	kWh	0.1~0.7	ΔSOC_{j}^{max}	kWh	5~10
$P_{j}^{Ch,max}$	kW	5~10	$P_{j}^{Dch,max}$	kW	5~10
η^{g2v}	%	95	η^{v2g}	%	95
χ	%	80~100	N^{max}	constant	10

The solar irradiation and wind speed data are adopted from [30, 31]. The DSO and MGO's electrical demands are illustrated in Figures 4 and 5.

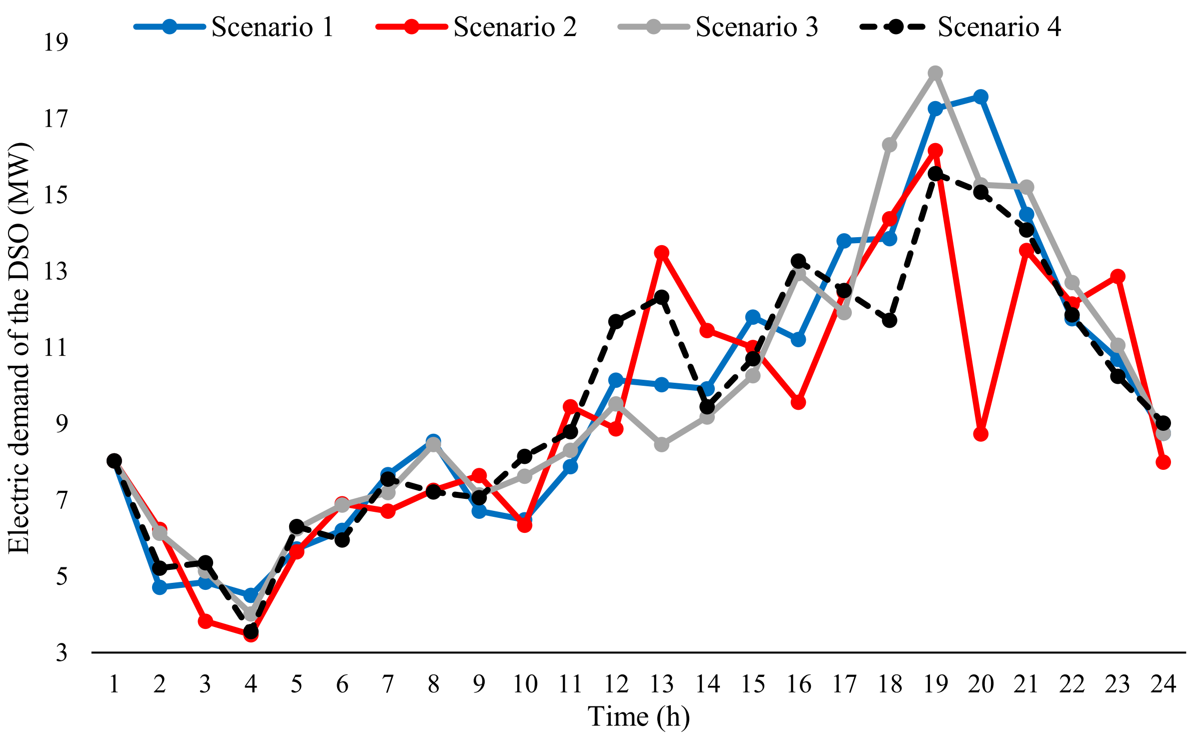

Fig. 4. Total electric demands of the DSO.

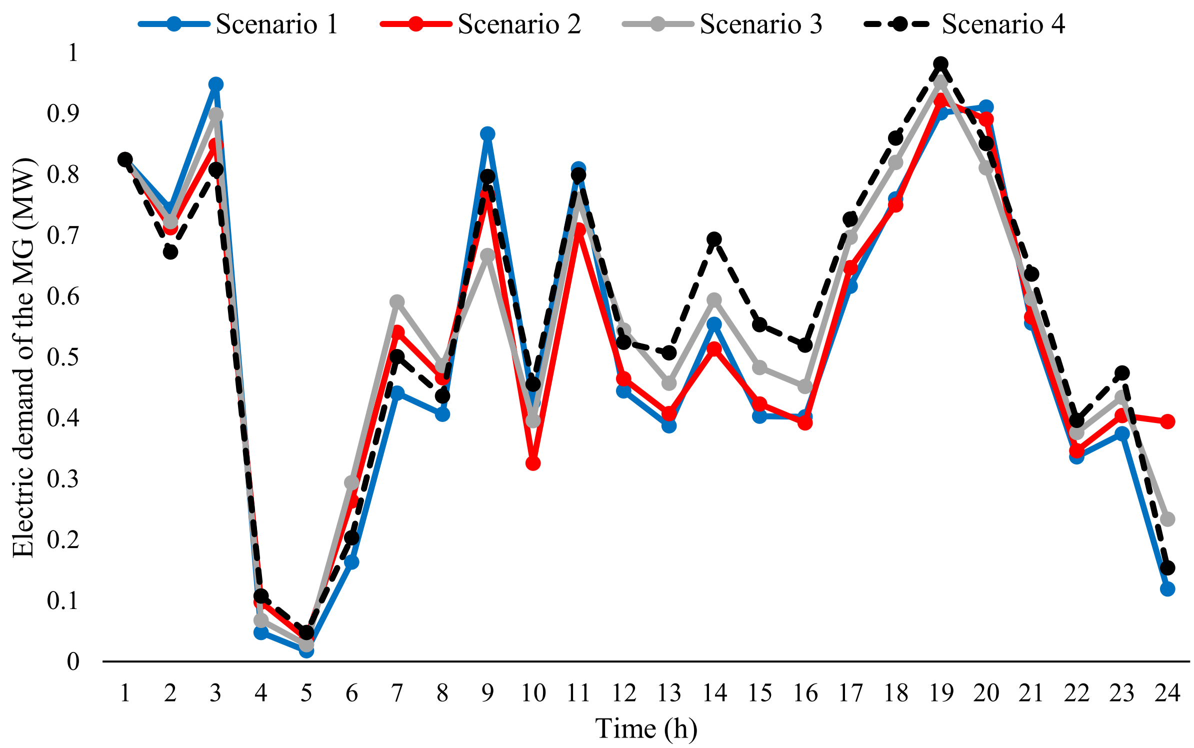

Fig. 5. Total electric demands of the MGO.

The wholesale and retail market prices, as well as the bilateral contract price between the DSO and MGO, are presented in Figure 6.

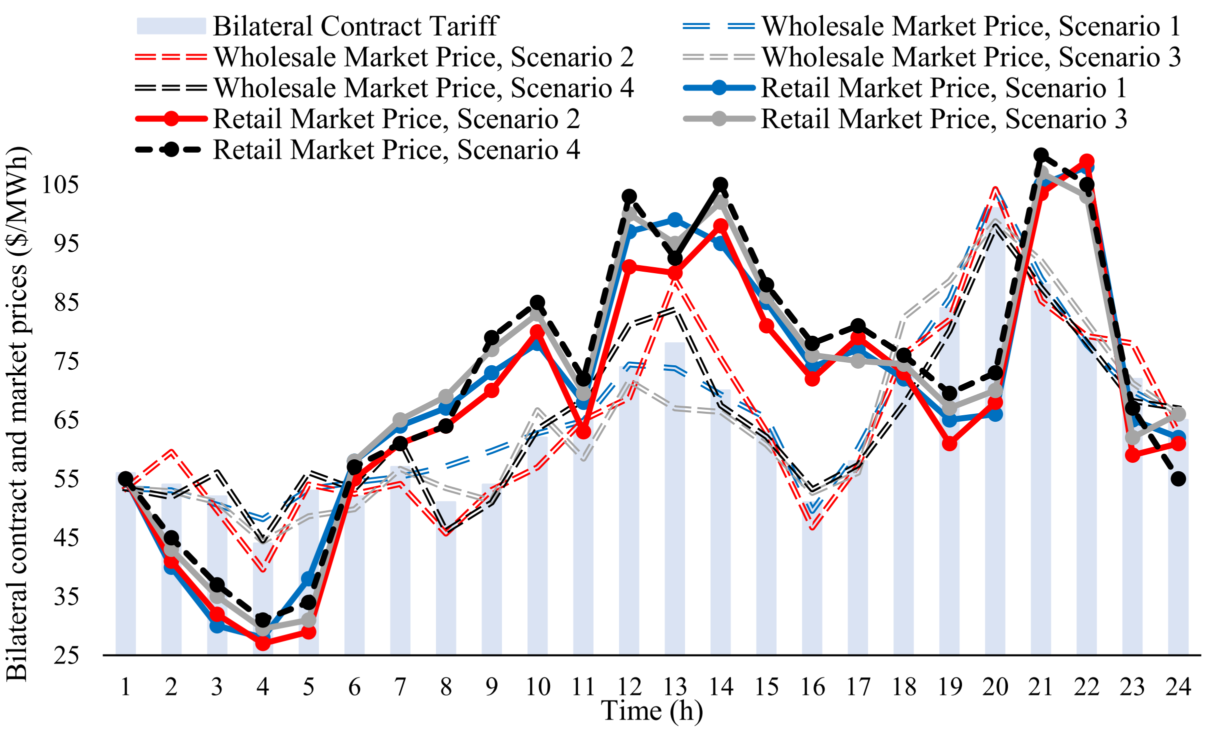

Fig. 6. Forecasted market prices and bilateral contract tariff.

Furthermore, the price of the scheduled reserve by the upper level's dispatchable units and CAES are considered to be 20% and 15% of their marginal energy production costs, respectively [41]. Also, the price of the committed reserve by the lower level's dispatchable units is considered to be 20% of their marginal energy production cost, and the price of the scheduled reserve by the eco-friendly IPL is assumed to be 10% of the discharge price of EVs. Finally, the forecasting errors of the wind speed and solar irradiance in both levels are considered to be 10%, and the forecasting error of total demands in both levels is considered to be 5%.

6.2. Results Analysis

The operation cost of the DSO and profit of the MGO in each case study are provided in Table 6.

Table 6: The DSO's operation cost and the MGO's profit in four studied cases.

	Case 1	Case 2	Case 3	Case 4
	$	$	$	$
Operation cost of the DSO	10710.111	10628.458	10638.722	10576.023
Differential in comparison to the Case 1 ($)		81.653	71.389	134.088
Profit of the MGO	659.455	832.921	1598.595	1566.389
Differential in comparison to the Case 1 ($)		173.466	939.14	906.934

For better comparison, obtained results of the first scenario in four cases are provided in the rest of the paper. At first, the detailed cost of each equipment in the first scenario is presented in Table 7.

Table 7: Operation cost of various equipment for scenario 1.

	Case 1	Case 2	Case 3	Case 4
	$	$	$	$
The upper level				
Cost of produced energy by the dispatchable units	9868.333	8493.364	9203.478	8550.866
Cost of scheduled reserve by the dispatchable units	281.964	266.037	272.036	242.123
Cost of produced energy by the CAES	X	26.500	X	28.812
Cost of scheduled reserve by the CAES	X	7.737	X	7.057
Cost of purchased energy from the wholesale market	1508.626	2480.796	1505.371	1836.939
Profit of sold energy to the wholesale market	2681.253	1860.111	2101.754	2032.885
Cost of purchased energy from the MGO	1834.575	1168.183	1841.299	1830.650
Profit of sold energy to the MGO	309.923	108.277	344.547	174.327
Cost of purchased reserve from the MGO	0	0.080	10.141	43.021
Profit of sold reserve to the MGO	137.364	154.366	134.278	78.143
The lower level				
Cost of produced energy by the dispatchable units	1065.427	431.650	1162.080	1233.055
Cost of scheduled reserve by the dispatchable units	11.028	10.805	7.441	17.230
Profit of sold energy to the IPL (Charge)	X	X	1663.307	1408.277

Cost of purchased energy from the IPL (Discharge)	✗	✗	635.473	342.434
Cost of purchased reserve from the IPL (Discharge)	✗	✗	16.401	30.889
Cost of purchased energy from the retail market	0	0	0	0
Profit of sold energy to the retail market	637.527	241.793	612.103	514.446
Cost of purchased energy from the DSO	309.923	108.277	344.547	174.327
Profit of sold energy to the DSO	1834.575	1168.183	1841.299	1830.650
Cost of purchased reserve from the DSO	137.364	154.366	134.278	78.143
Profit of sold reserve to the DSO	0	0.080	10.141	43.021

Detailed scheduled energy and reserve by each equipment during the 24 h in the first scenario of four cases are provided in Table 8.

Table 8: Scheduled energy/reserve by different equipment during the 24 h.

	Case 1	Case 2	Case 3	Case 4
	MWh	MWh	MWh	MWh
The upper level				
Produced energy by the WTs	279.557	279.557	279.557	279.557
Produced energy by the PVs	65.273	65.273	65.273	65.273
Produced energy by the dispatchable units	522.638	479.595	490.561	466.737
Scheduled reserve by the dispatchable units	90.745	85.339	87.731	83.868
Charge rate of the CAES	✗	15.286	✗	15.306
Discharge rate of the CAES	✗	8.199	✗	9.260
Scheduled reserve by the CAES	✗	4.076	✗	3.034
Imported energy from the wholesale market	150.227	167.554	151.088	168.656
Exported energy to the wholesale market	165.494	154.826	157.198	146.766
Imported energy from the MG	76.494	95.718	100.369	99.177
Exported energy to the MG	7.253	4.342	8.209	5.146
Imported reserve from the MG	0.026	0.085	0.893	1.382
Exported reserve to the MG	10.216	8.945	8.070	7.729
The lower level				
Produced energy by the WTs	86.126	86.126	86.126	86.126
Produced energy by the PVs	12.862	12.862	12.862	12.862
Produced energy by the dispatchable units	40.622	60.917	74.812	75.379
Scheduled reserve by the dispatchable units	2.292	3.622	3.465	4.060
Charge rate of the IPL	✗	✗	20.760	20.112
Discharge rate of the IPL	✗	✗	10.844	10.037
Scheduled reserve by the IPL	✗	✗	1.842	2.076
Imported energy from the retail market	0.420	0.420	1.046	1.120
Exported energy to the retail market	19.109	17.270	21.090	19.701
Imported energy from the DSO	7.253	4.342	8.209	5.146
Exported energy to the DSO	76.494	95.718	100.369	99.177
Imported reserve from the DSO	10.216	8.945	8.070	7.729
Exported reserve to the DSO	0.026	0.085	0.893	1.382

Scheduled power and reserve by dispatchable units of the DSO are shown in Figures 7 and 8, respectively. Produced energy by the mentioned units in the second, third, and fourth case studies is reduced by 8.24%, 6.14%, and 10.7% in comparison to the case 1. The mentioned units similarly provide the reserve capacity. In other words, the scheduled reserve is decreased by 5.96%, 3.32%, and 7.58% in case studies 2-4 in comparison to case study 1. Also, it can be realized that the dispatchable units start providing power and reserve from the hours that the market price starts to increase drastically.

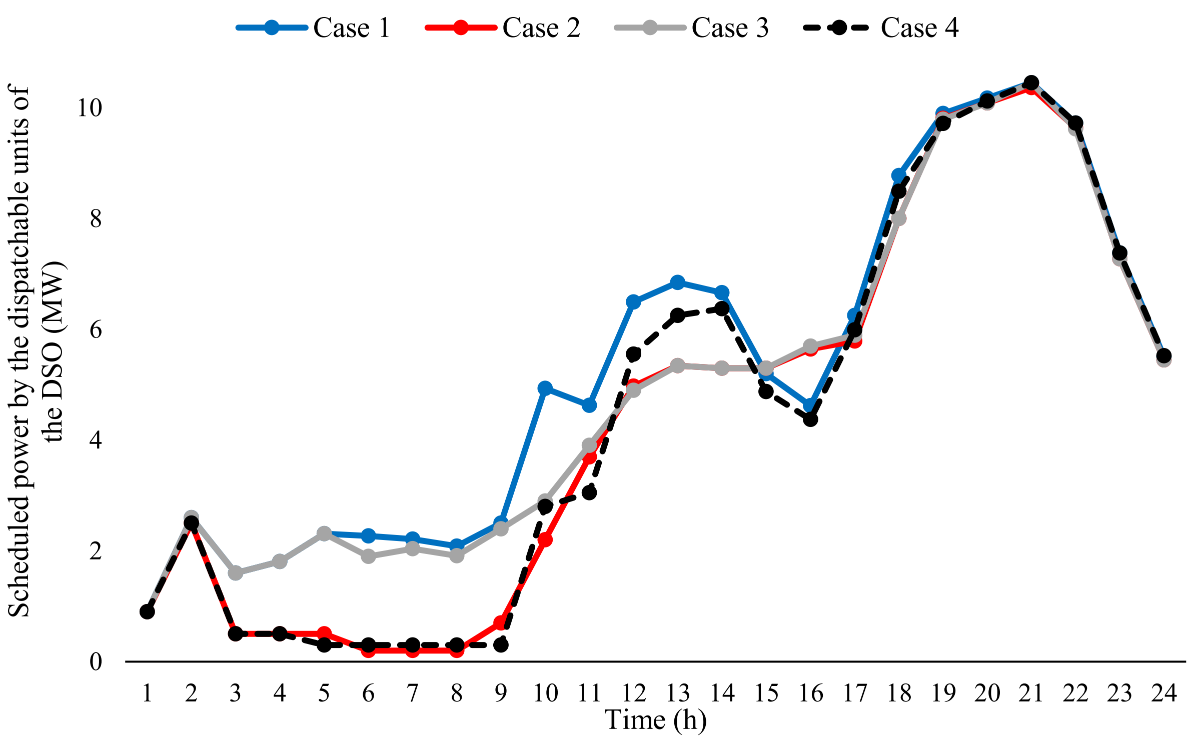

Fig. 7. Scheduled power by the DSO's dispatchable units.

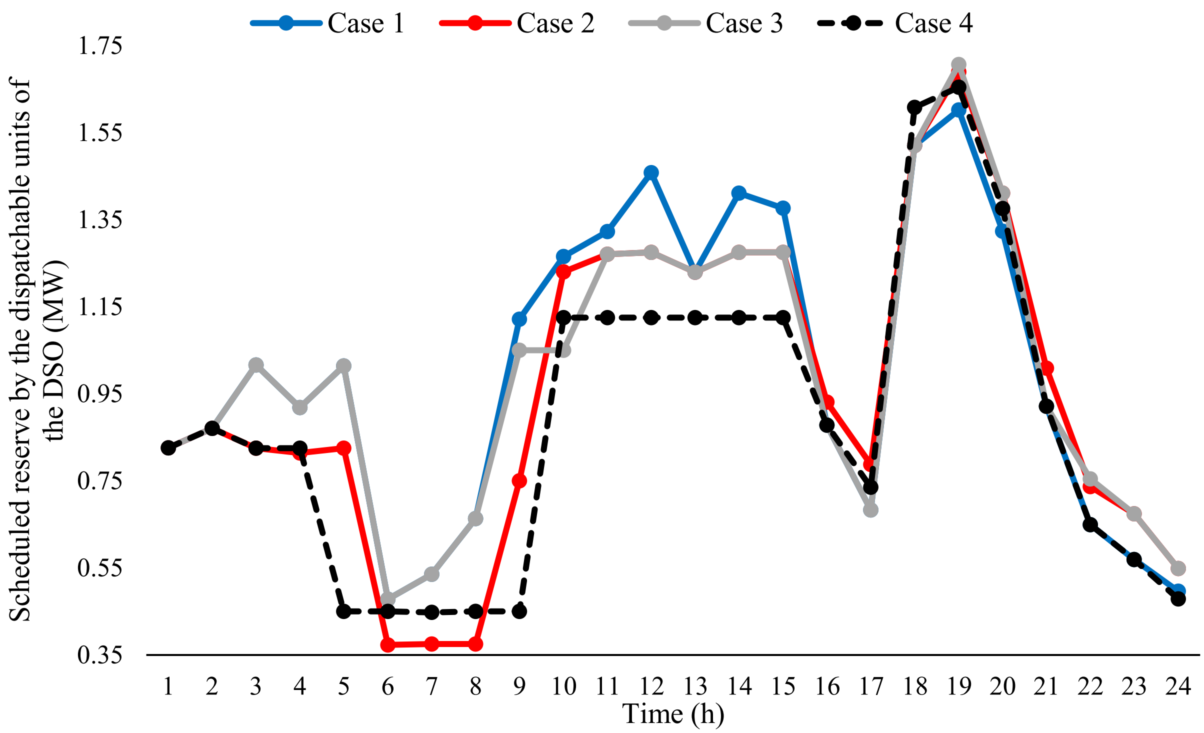

Fig. 8. Scheduled reserve by the DSO's dispatchable units.

Scheduled power and reserve by the dispatchable units of the MGO are presented in Figures 9 and 10, respectively. According to the reported results, produced power by the dispatchable units is increased significantly in the presence of the CAES and IPL. For example, produced energy by the mentioned units is increased by 49.96%, 84.17%, and 85.56%, respectively, in cases 2-4 in comparison to case study 1. Scheduled reserve by the units, as mentioned above, is increased by 58.03%, 51.18%, and 77.14%, respectively, in case studies 2-4. Thus, it can be concluded that the portion of the reserve and energy procurement is increased significantly, which makes the MGO earn more profit through selling the scheduled energy and reserve to the retail market and the DSO.

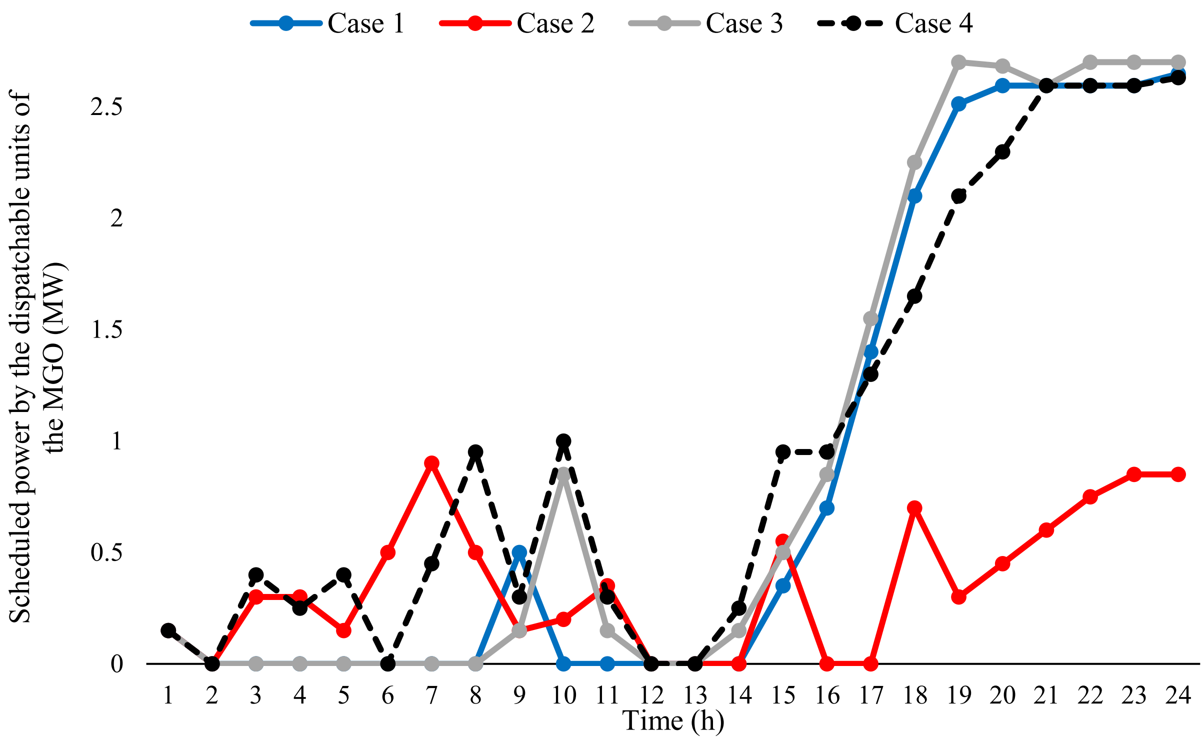

Fig. 9. Scheduled power by the MGO's dispatchable units.

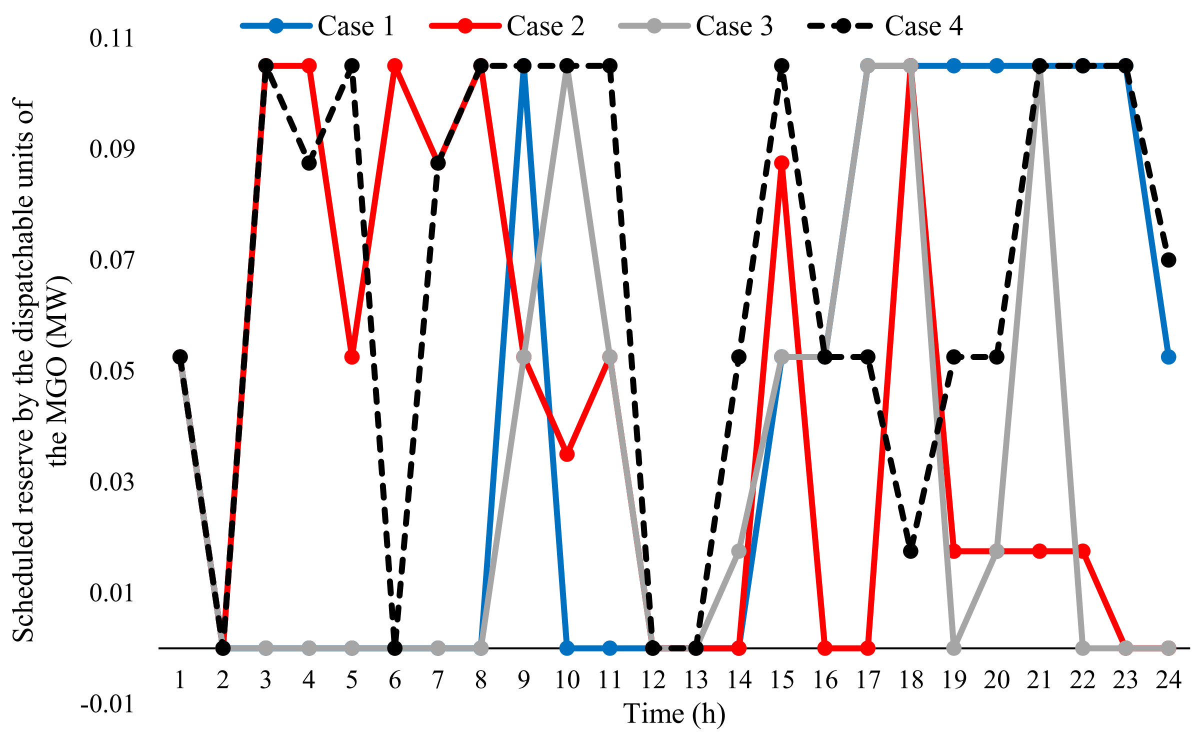

Fig. 10. Scheduled reserve by the MGO's dispatchable units.

Charge and discharge rates of the CAES and scheduled reserve by this equipment are presented in Figures 11 and 12, respectively. By analyzing the results of cases 2 and 4, it can be realized that charge and discharge rates of the CAES is increased 0.13%, and 12.94% in the presence of IPL, while the amount of scheduled reserve by this unit is decreased 25.56%. The CAES starts to discharge from the hour 18 to 21, in which the market price starts to be increased and reached its peak at hour 20. At the mentioned hour, the CAES tries to discharge power as much as possible. Scheduled reserve by the CAES peaked at nearly 420 kW at hour 9 in case 2 and approximately 470 kW at the same time in case 4.

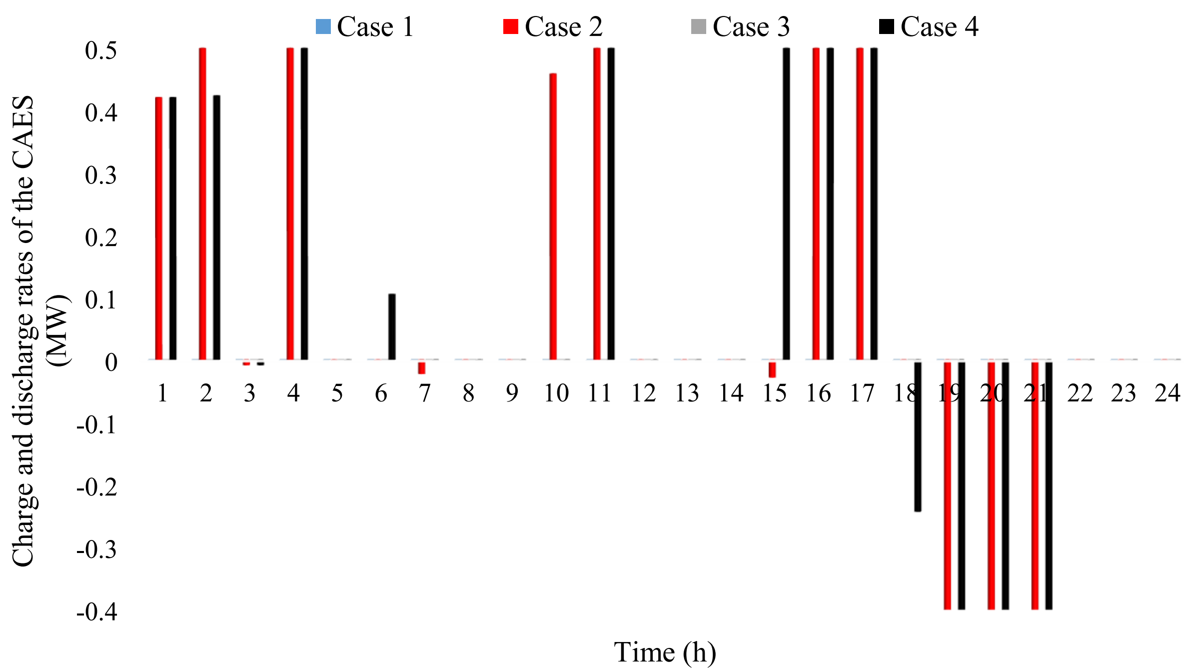

Fig. 11. Charge and discharge rates of the CAES.

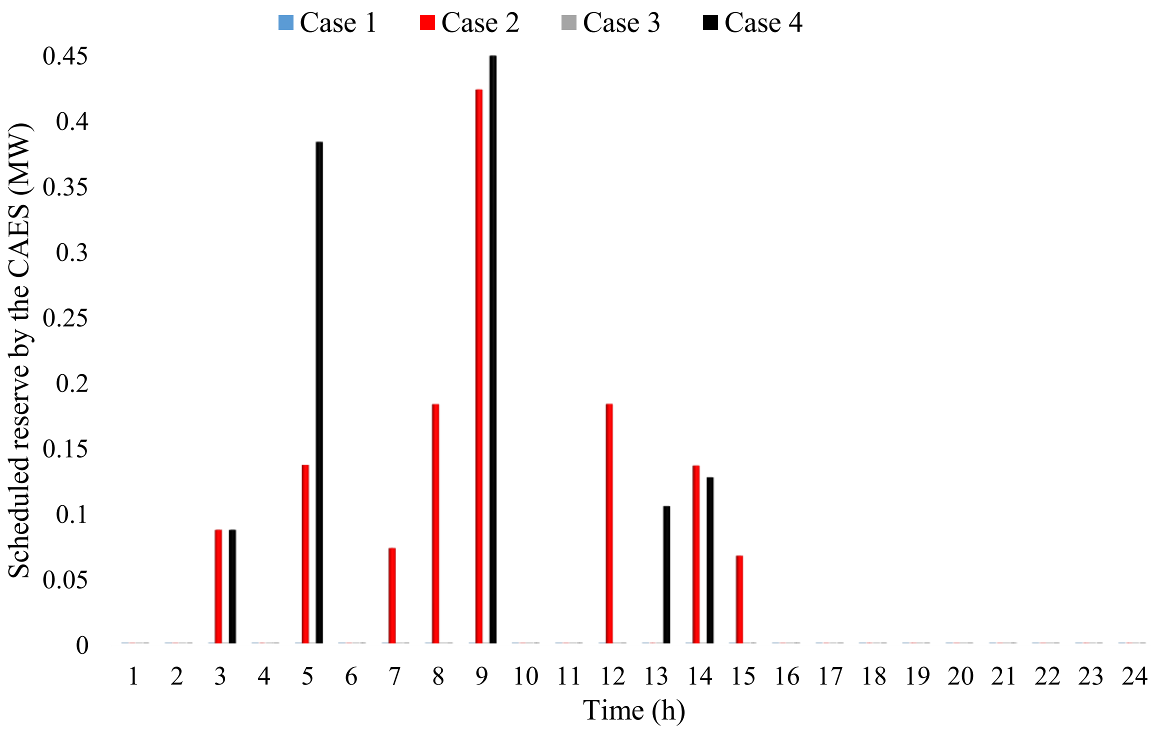

Fig. 12. Scheduled reserve by the CAES.

Charge and discharge rates of the IPL, as well as the scheduled reserve by the mentioned unit, are illustrated in Figures 13 and 14, respectively. By comparing the obtained results of cases 3 and 4, it can be seen that the charge, discharge rates are decreased by 3.12%, and 7.44% in the presence of both CAES and IPL. The scheduled reserve by the IPL is increased by 12.7% in case 4 in comparison to case 3. By analyzing the obtained results in detail, it can be realized that the portion of the scheduled reserve by the IPL peak at nearly 180 kW and nearly 330 kW at hour 12, in cases 3 and 4. Furthermore, the charge rate is more than the discharge rate, which makes the MGO gain profit as much as possible.

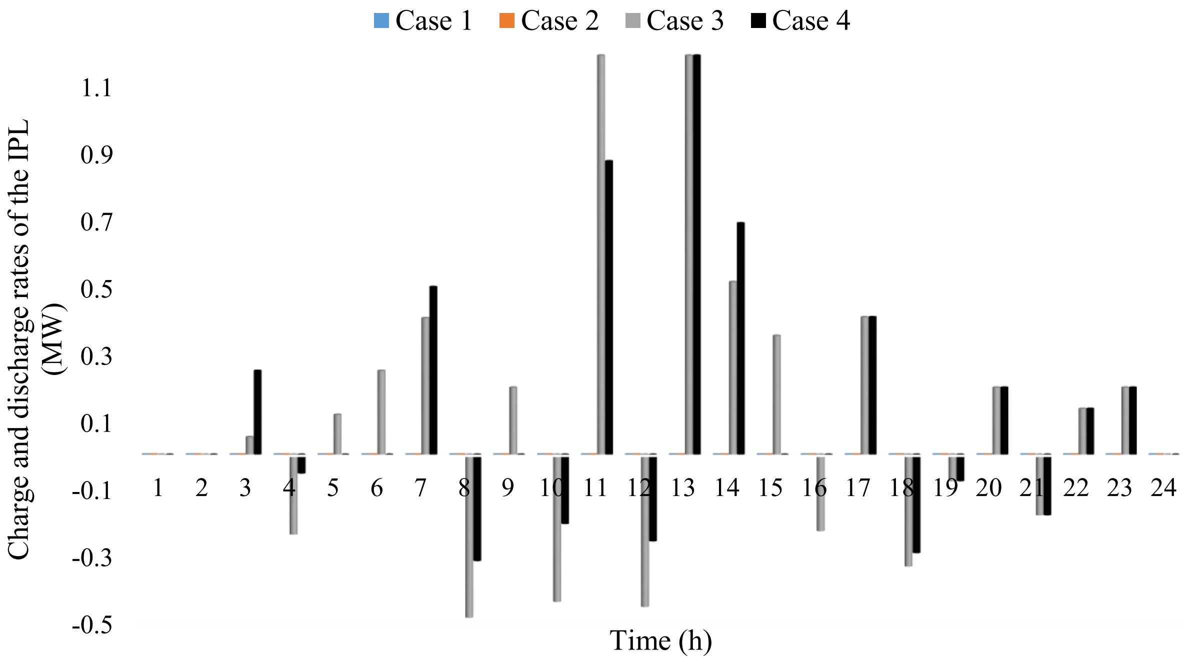

Fig. 13. Charge and discharge rates of the IPL.

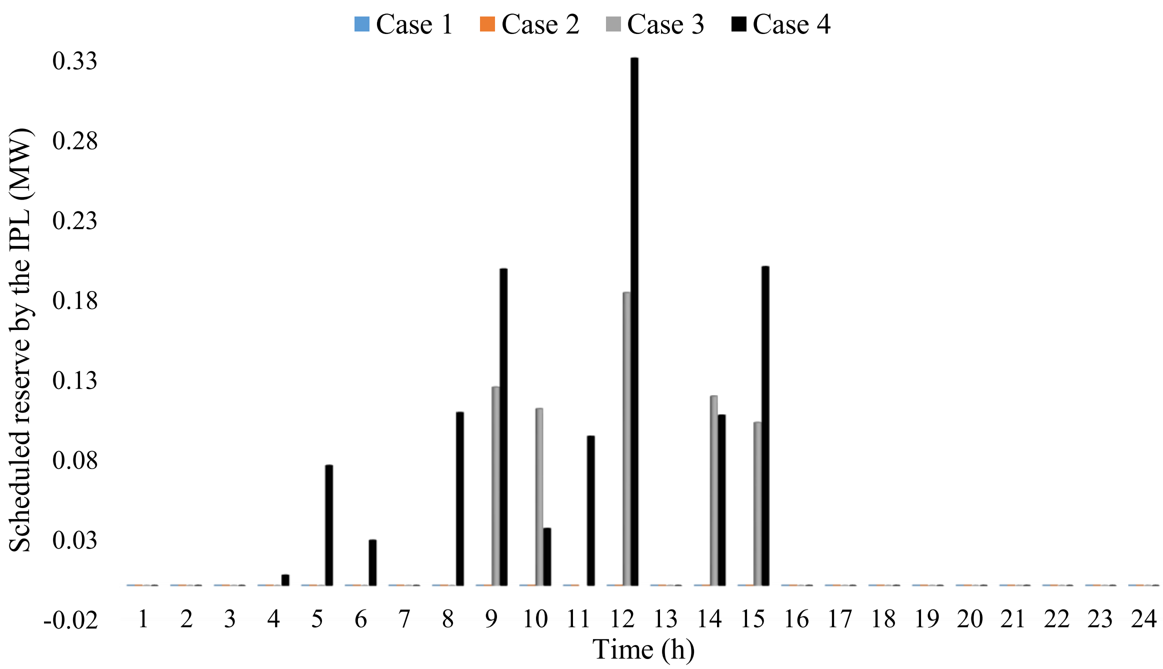

Fig. 14. Scheduled reserve by the IPL.

Exchanged power between the MGO and retail market, as well as exchanged power between the DSO and wholesale market, are illustrated in Figures 15 and 16, respectively. Furthermore, exchanged power and reserve between the DSO and MGO, from the DSO's points of view, are illustrated in Figures 17 and 18, respectively.

The imported power from the retail market, from the MGO's perspective, is marginal during the studied period. The imported energy remained constant in case 2 in comparison to case 1, around 420 kWh. The amount of imported energy is increased by approximately 626 kWh, from 0.420 MWh to 1.046 MWh, in case 3 and increased 700 kWh, from 0.42 MWh to 1.12 MWh, in the presence of both IPL and CAES. The amount of exported energy to the retail market, from the MGO's perspective, is decreased 9.62% in case 2 and increased 10.37% and 3.1% in cases 3 and 4 in comparison to the case 1.

The amount of imported energy from the wholesale market, from the DSO's perspective, is increased by 11.53%, 0.57%, and 12.27%, respectively, in cases 2-4 in comparison to case 1. On the other hand, the amount of exported energy to the wholesale market, from the DSO's perspective, is decreased by 6.54%, 5.01%, and 11.32%, respectively, in cases 2-4. The produced power by the dispatchable units reaches their maximum production capacity during the hours 9-15 and 17-23. The produced power during the first period, hours 9-15, is sold to the wholesale market that makes the operation cost of the DSO to be decreased. In the second period, hours 17-23, due to the high level of the electric demand, a large portion of the produced power by the dispatchable units is used to meet the demand, and the capability of purchasing power from the wholesale market is used to fulfill the rest of the unserved demand. Also, it can be seen that at hours 12 or 14, since the wholesale market price is higher than the marginal generation costs of DSO's dispatchable units, the DSO has preferred to exploit these units to sell more power to the market.

The amount of imported energy from the MG, from the DSO's perspective, is increased by 25.13%, 31.21%, and 29.65% in cases 2-4 in comparison to case 1. The amount of exported energy to the MG, from the DSO's perspective, is decreased by 40.14%, 29.05% with considering the CAES and both CAES and IPL, respectively. In case 3, the limitation of the MGO's dispatchable units make the MGO purchase approximately 2.61 MW at hour 3 and 2.21 MW at hour 5 from the DSO. The portion of the purchased energy from the DSO is decreased in case 4 in comparison to case 1. So, the presence of the IPL makes the MGO gain a little bit more profit. After hour 6, the electric demand of the DSO is increased, which makes the DSO meet the portion of its demand by purchasing the electric power from the MGO.

The imported reserve from the MGO, from the DSO's perspective, is increased 1356 kWh, from 0.026 MWh to 1.382 MWh, in case 4 in comparison to case 1. The amount of imported reserve is increased by 59 kWh and 867 kWh in cases 2 and 3 in comparison to case 1. Finally, the amount of exported reserve to the MGO, from the DSO's perspective, is decreased 1271 kWh, from 10.216 MWh to 8.945 MWh, with considering the CAES, and 2146 kWh, from 10.216 MWh to 8.07 MWh, with considering the IPL, and 2487 kWh, from 10.216 MWh to 7.729 MWh, with considering both IPL and CAES. In cases 1 and 2, due to the absence of the IPL and own small-sized dispatchable units, MGO has to import a large portion of the reserve demand from the DSO. In cases 3 and 4, the MGO took advantage of the IPL and sold the portion of its scheduled reserve to the DSO. The sold reserve to the DSO is peaked at 190 kW during the hour 9 and reach a high of 150 kW and 140 kW in case 4, during the hours 12, and 15, respectively.

It should be noted that imported power/reserve from the wholesale market/MGO, from the DSO's perspective, is considered to be positive. In contrast, the exported power/reserve to the wholesale market/MGO is considered to be negative.

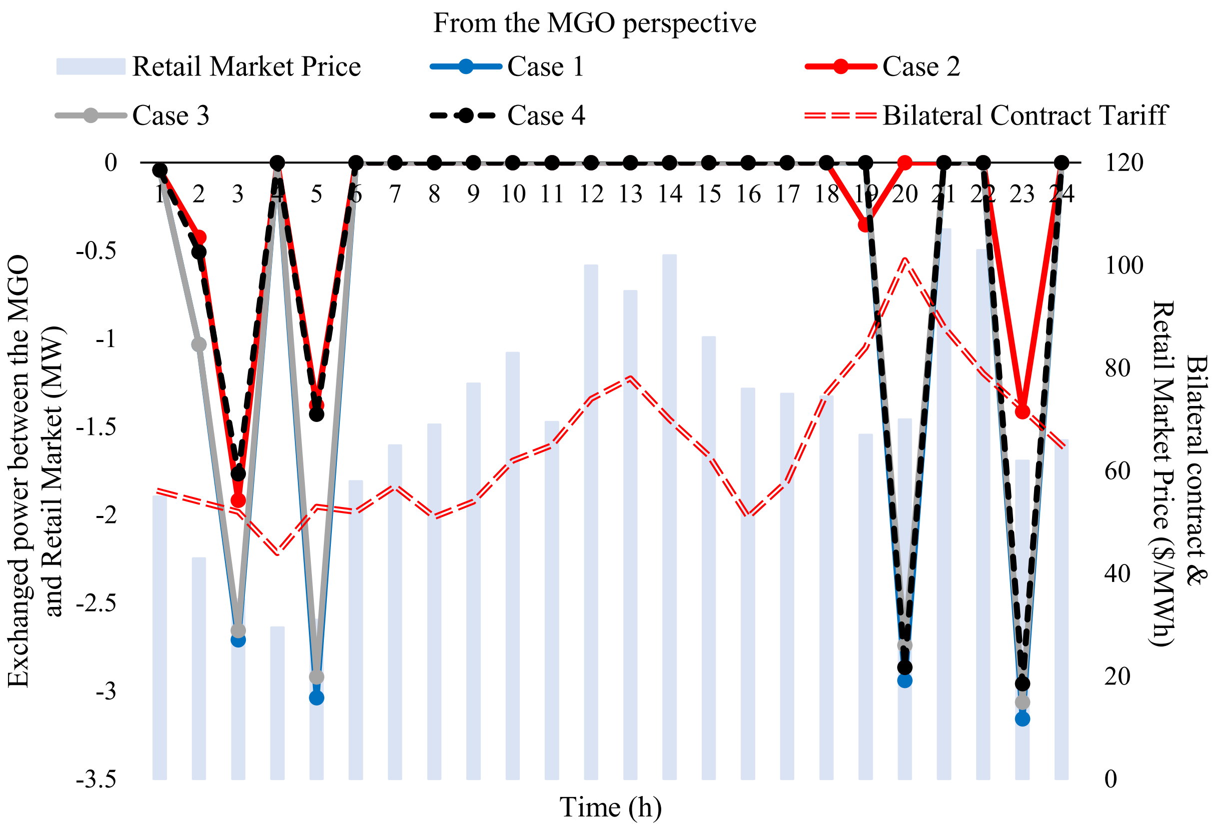

Fig. 15. Exchanged power between the MGO and retail market from the MGO's viewpoint.

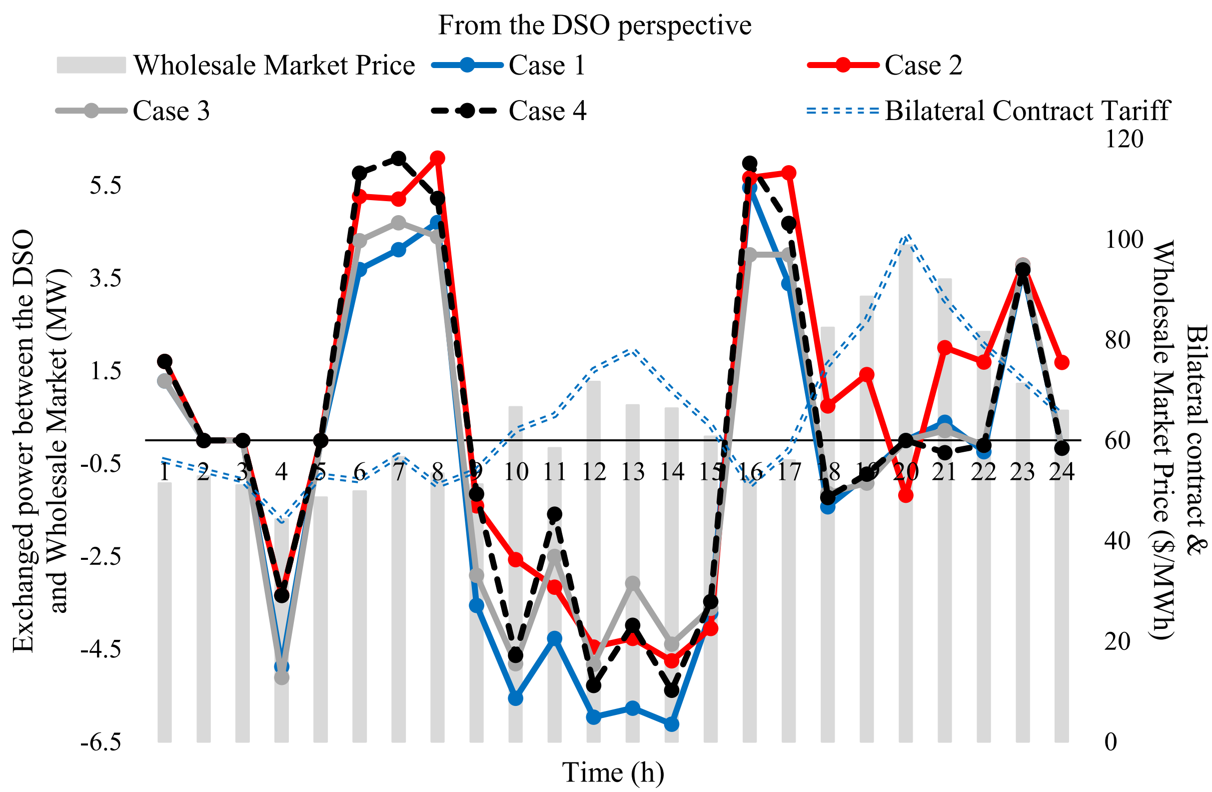

Fig. 16. Exchanged power between the DSO and wholesale market from the DSO's viewpoint.

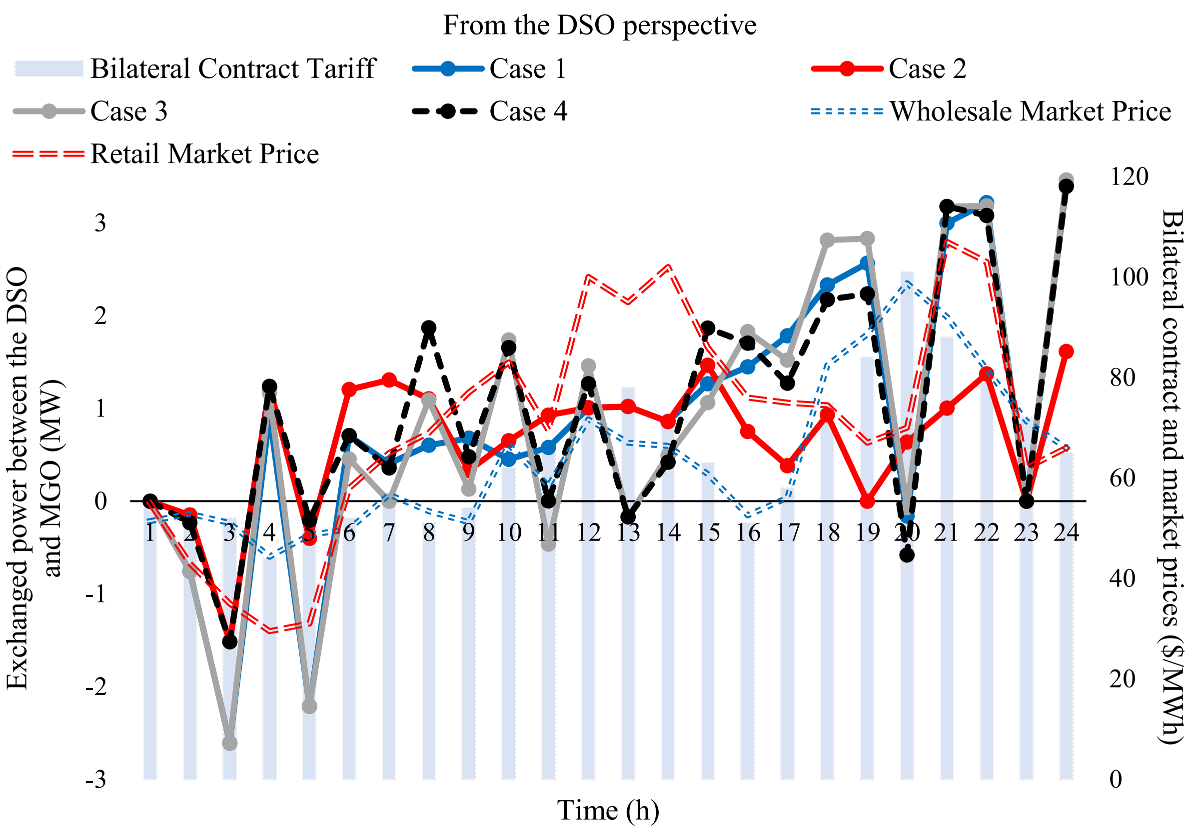

Fig. 17. Exchanged power between the DSO and MGO from the DSO's viewpoints

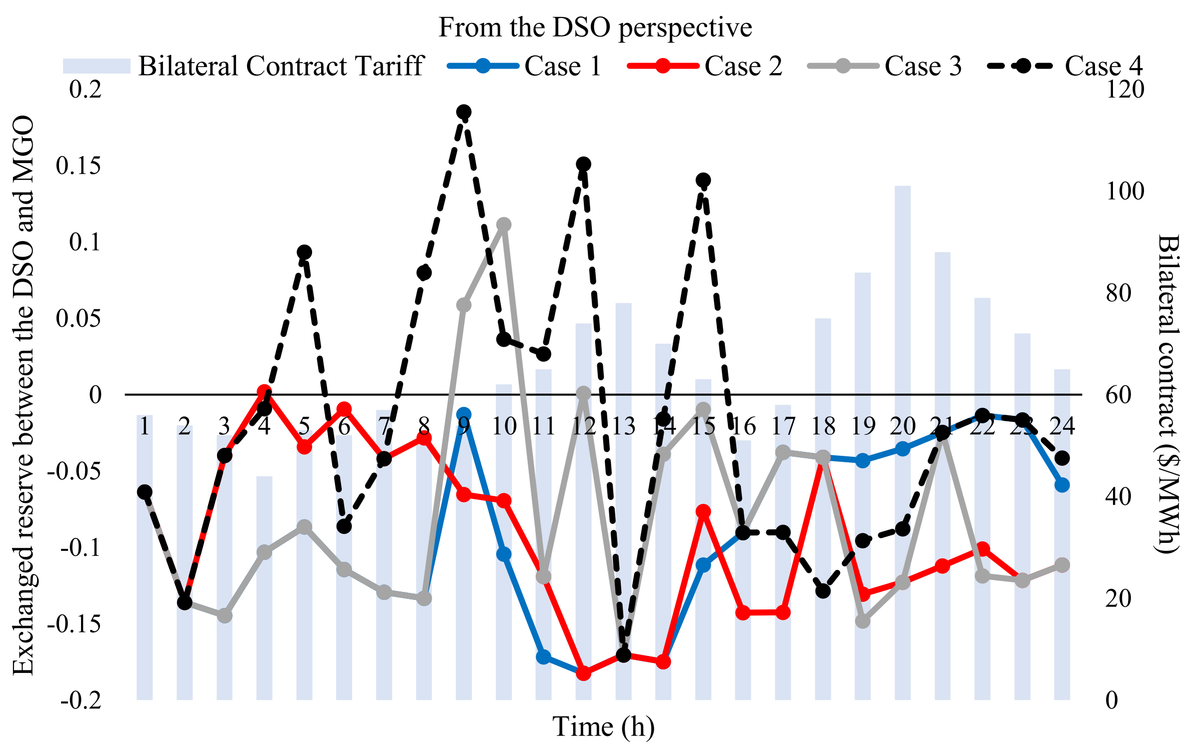

Fig. 18. Exchanged reserve between the DSO and MGO from the DSO's viewpoint.

In the end, to prove the superiority of the proposed bi-level stochastic programming framework, this model is compared with a single-level model. In the considered single-level model, the optimal scheduling of the studied ADS is only executed form the DSO's perspective. Indeed, in this situation, the MGO's objective function is neglected. Obtained results from these two cases are compared with one another in Table 9.

Table 9: Comparison between the bi-level and single-level models

	Bi-Level Model	Single-Level model	Percentage Decrease
	$	$	%
Total Operating Cost of the DSO	10576.023	10017.338	-5.28
Expected Profit of the MGO	1566.389	1086.761	-30.62

As it is clear, by scheduling the studied ADS from the DSO's standpoint, its operating cost is decreased by up 558.685 $, 5.28%. In contrast, the MGO's profit is reduced up to 479.628 $, 30.62%, as well. Among the presented answers, the DSO would prefer the condition in which it has the minimum operating cost. Nonetheless, this situation could not be in the best interest of the MGO. As a result, the proposed bi-level model can provide a win-win situation for both considered players.

7. Conclusion

In this paper, the day-ahead scheduling of the DSO that plays the role of the leader, and independent renewable-based MGO that plays the role of the follower, was optimized under distribution network constraints through a stochastic bi-level programming model. The capability of exchanging power and reserve between the MGO and DSO is considered in this paper, too. The considered DSO model was comprised of dispatchable units, and clean energy production units such as WTs, PVs, and CAES. Also, the considered MGO model was comprised of dispatchable units, and some environmentally sound units such as WTs, PVs, and IPL. The proposed model was analyzed in four case studies with and without considering the eco-friendly units, IPL, and CAES. According to the obtained results, it can be realized that the operation cost of the DSO without CAES and IPL was about 10710.111$, in which the mentioned cost could be reduced up to 134.09$ by considering both CAES and IPL at the same time. On the other hand, from the MGO's perspective, it can be seen that the profit of the MGO was increased 173.47$ without considering the carbon-neutral IPL, and 939.14$ with considering IPL, and 906.93$ with considering both CAES and IPL. As a result, it can be concluded that the IPL and CAES that play the role of environmentally-friendly and large-scale storage systems could increase the resistance of the system, decrease the operation cost and maximize the profit of the existing independent players.

Ultimately, the following issues are presented as future works:

1. The risk-constraint scheduling of the provided bi-level model with the use of the conditional value at risk approach.

2. Considering several private renewable-based MGOs or some clean energy production IPLs and modeling their interactions through the multi follower bi-level programming.

3. Studying the stochastic behavior of the EVs' owners under economic and climate-friendly constrains.

Acknowledgement

The work of M. Shafie-khah was carried out in SolarX research project with financial support provided by the Business Finland, 2019-2021 (grant No. 6844/31/2018).

References

[1] E. Rakhshani, H. Mehrjerdi, and A. Iqbal, "Hybrid wind-diesel-battery system planning considering multiple different wind turbine technologies installation," *Journal of Cleaner Production,* vol. 247, p. 119654, 2020.

[2] C. Li, H. Zhou, J. Li, and Z. Dong, "Economic dispatching strategy of distributed energy storage for deferring substation expansion in the distribution network with distributed generation and electric vehicle," *Journal of Cleaner Production,* p. 119862, 2020.
[3] T. Castillo-Calzadilla, A. M. Macarulla, O. Kamara-Esteban, and C. E. Borges, "A case study comparison between photovoltaic and fossil generation based on direct current hybrid microgrids to power a service building," *Journal of Cleaner Production,* vol. 244, p. 118870, 2020.
[4] Z. Wang, P. Jochem, and W. Fichtner, "A scenario-based stochastic optimization model for charging scheduling of electric vehicles under uncertainties of vehicle availability and charging demand," *Journal of Cleaner Production,* vol. 254, p. 119886, 2020.
[5] S. Haghifam, M. Dadashi, K. Zare, and H. Seyedi, "Optimal operation of smart distribution networks in the presence of demand response aggregators and microgrid owners: A multi follower Bi-Level approach," *Sustainable Cities and Society,* vol. 55, p. 102033, 2020.
[6] B. Aluisio, A. Conserva, M. Dicorato, G. Forte, and M. Trovato, "Optimal operation planning of V2G-equipped Microgrid in the presence of EV aggregator," *Electric Power Systems Research,* vol. 152, pp. 295-305, 2017.
[7] M. Mohiti, H. Monsef, and H. Lesani, "A decentralized robust model for coordinated operation of smart distribution network and electric vehicle aggregators," *International Journal of Electrical Power & Energy Systems,* vol. 104, pp. 853-867, 2019.
[8] A. Zakariazadeh, S. Jadid, and P. Siano, "Smart microgrid energy and reserve scheduling with demand response using stochastic optimization," *International Journal of Electrical Power & Energy Systems,* vol. 63, pp. 523-533, 2014.
[9] M. Ghahramani, M. Nazari-Heris, K. Zare, and B. Mohammadi-Ivatloo, "Energy and Reserve Management of a Smart Distribution System by Incorporating Responsive-Loads/Battery/Wind Turbines Considering Uncertain Parameters," *Energy,* 2019.
[10] M. Zhang, X. Ai, J. Fang, and J. Wen, "Two-stage stochastic programming for the joint dispatch of energy and reserve considering demand response," *The Journal of Engineering,* vol. 2019, no. 18, pp. 5172-5177, 2019.
[11] M. Mohiti, H. Monsef, A. Anvari-Moghaddam, J. Guerrero, and H. Lesani, "A decentralized robust model for optimal operation of distribution companies with private microgrids," *International Journal of Electrical Power & Energy Systems,* vol. 106, pp. 105-123, 2019.
[12] S. M. B. Sadati, J. Moshtagh, M. Shafie-khah, and J. P. Catalão, "Smart distribution system operational scheduling considering electric vehicle parking lot and demand response programs," *Electric Power Systems Research,* vol. 160, pp. 404-418, 2018.
[13] M. A. Mirzaei, A. S. Yazdankhah, B. Mohammadi-Ivatloo, M. Marzband, M. Shafie-khah, and J. P. Catalão, "Stochastic network-constrained co-optimization of energy and reserve products in renewable energy integrated power and gas networks with energy storage system," *Journal of Cleaner Production,* vol. 223, pp. 747-758, 2019.
[14] J. Salehi and A. Abdolahi, "Optimal scheduling of active distribution networks with penetration of PHEV considering congestion and air pollution using DR program," *Sustainable Cities and Society,* vol. 51, p. 101709, 2019.
[15] J. Jannati and D. Nazarpour, "Optimal performance of electric vehicles parking lot considering environmental issue," *Journal of cleaner production,* vol. 206, pp. 1073-1088, 2019.
[16] P. Aliasghari, B. Mohammadi-Ivatloo, M. Alipour, M. Abapour, and K. Zare, "Optimal scheduling of plug-in electric vehicles and renewable micro-grid in energy and reserve markets considering demand response program," *Journal of Cleaner Production,* vol. 186, pp. 293-303, 2018.
[17] S. S. Barhagh, B. Mohammadi-Ivatloo, A. Anvari-Moghaddam, and S. Asadi, "Risk-involved participation of electric vehicle aggregator in energy markets with robust decision-making approach," *Journal of Cleaner Production,* vol. 239, p. 118076, 2019.
[18] S. M. B. Sadati, J. Moshtagh, M. Shafie-khah, A. Rastgou, and J. P. Catalão, "Operational scheduling of a smart distribution system considering electric vehicles parking lot: A bi-level

approach," *International Journal of Electrical Power & Energy Systems,* vol. 105, pp. 159-178, 2019.
[19] S. Esmaeili, A. Anvari-Moghaddam, and S. Jadid, "Optimal Operational Scheduling of Reconfigurable Multi-Microgrids Considering Energy Storage Systems," *Energies,* vol. 12, no. 9, p. 1766, 2019.
[20] S. Bahramara, M. P. Moghaddam, and M. Haghifam, "A bi-level optimization model for operation of distribution networks with micro-grids," *International Journal of Electrical Power & Energy Systems,* vol. 82, pp. 169-178, 2016.
[21] T. Lv, Q. Ai, and Y. Zhao, "A bi-level multi-objective optimal operation of grid-connected microgrids," *Electric Power Systems Research,* vol. 131, pp. 60-70, 2016.
[22] M. Moradijoz, M. P. Moghaddam, and M.-R. Haghifam, "A flexible distribution system expansion planning model: a dynamic bi-level approach," *IEEE Transactions on Smart Grid,* vol. 9, no. 6, pp. 5867-5877, 2017.
[23] S. M. B. Sadati, J. Moshtagh, M. Shafie-khah, A. Rastgou, and J. P. Catalão, "Bi-level model for operational scheduling of a distribution company that supplies electric vehicle parking lots," *Electric Power Systems Research,* vol. 174, p. 105875, 2019.
[24] L. Ju, Z. Tan, J. Yuan, Q. Tan, H. Li, and F. Dong, "A bi-level stochastic scheduling optimization model for a virtual power plant connected to a wind–photovoltaic–energy storage system considering the uncertainty and demand response," *Applied energy,* vol. 171, pp. 184-199, 2016.
[25] M. Jalali, K. Zare, and H. Seyedi, "Strategic decision-making of distribution network operator with multi-microgrids considering demand response program," *Energy,* vol. 141, pp. 1059-1071, 2017.
[26] M. Alipour, K. Zare, and H. Seyedi, "A multi-follower bilevel stochastic programming approach for energy management of combined heat and power micro-grids," *Energy,* vol. 149, pp. 135-146, 2018.
[27] S. Aghajani and M. Kalantar, "Operational scheduling of electric vehicles parking lot integrated with renewable generation based on bilevel programming approach," *Energy,* vol. 139, pp. 422-432, 2017.
[28] S. Nojavan and H. allah Aalami, "Stochastic energy procurement of large electricity consumer considering photovoltaic, wind-turbine, micro-turbines, energy storage system in the presence of demand response program," *Energy Conversion and Management,* vol. 103, pp. 1008-1018, 2015.
[29] H. Khaloie *et al.*, "Co-optimized bidding strategy of an integrated wind-thermal-photovoltaic system in deregulated electricity market under uncertainties," *Journal of Cleaner Production,* vol. 242, p. 118434, 2020.
[30] A. N. Ghalelou, A. P. Fakhri, S. Nojavan, M. Majidi, and H. Hatami, "A stochastic self-scheduling program for compressed air energy storage (CAES) of renewable energy sources (RESs) based on a demand response mechanism," *Energy Conversion and Management,* vol. 120, pp. 388-396, 2016.
[31] M. Honarmand, A. Zakariazadeh, and S. Jadid, "Integrated scheduling of renewable generation and electric vehicles parking lot in a smart microgrid," *Energy Conversion and Management,* vol. 86, pp. 745-755, 2014.
[32] A. Meeraus, M. Bussieck, J.-H. Jagla, F. Nelissen, and L. Westermann, *GAMS*. Scientific Press, 1988.
[33] A. Sinha, P. Malo, and K. Deb, "A review on bilevel optimization: From classical to evolutionary approaches and applications," *IEEE Transactions on Evolutionary Computation,* vol. 22, no. 2, pp. 276-295, 2017.
[34] A. Zakariazadeh, S. Jadid, and P. Siano, "Economic-environmental energy and reserve scheduling of smart distribution systems: A multiobjective mathematical programming approach," *Energy Conversion and Management,* vol. 78, pp. 151-164, 2014.
[35] S. Talari, M. Shafie-Khah, F. Wang, J. Aghaei, and J. P. Catalão, "Optimal scheduling of demand response in pre-emptive markets based on stochastic bilevel programming method," *IEEE Transactions on Industrial Electronics,* vol. 66, no. 2, pp. 1453-1464, 2017.

[36] M. Jadidbonab, E. Babaei, and B. Mohammadi-ivatloo, "CVaR-constrained scheduling strategy for smart multi carrier energy hub considering demand response and compressed air energy storage," *Energy,* vol. 174, pp. 1238-1250, 2019.
[37] E.-G. Talbi, "A taxonomy of metaheuristics for bi-level optimization," in *Metaheuristics for bi-level optimization*: Springer, 2013, pp. 1-39.
[38] J. Lu, C. Shi, G. Zhang, and T. Dillon, "Model and extended Kuhn–Tucker approach for bilevel multi-follower decision making in a referential-uncooperative situation," *Journal of Global Optimization,* vol. 38, no. 4, pp. 597-608, 2007.
[39] S. J. Kazempour, A. J. Conejo, and C. Ruiz, "Strategic generation investment using a complementarity approach," *IEEE Transactions on Power Systems,* vol. 26, no. 2, pp. 940-948, 2010.
[40] S. Haghifam, K. Zare, and M. Dadashi, "Bi-level operational planning of microgrids with considering demand response technology and contingency analysis," *IET Generation, Transmission & Distribution,* 2019.
[41] F. Bouffard, F. D. Galiana, and A. J. Conejo, "Market-clearing with stochastic security-part II: case studies," *IEEE Transactions on Power Systems,* vol. 20, no. 4, pp. 1827-1835, 2005.